Hunt for light primordial black hole dark matter with UHF-GWs

Quantum Technologies for Fundamental Physics

Erice - 05/09/2023

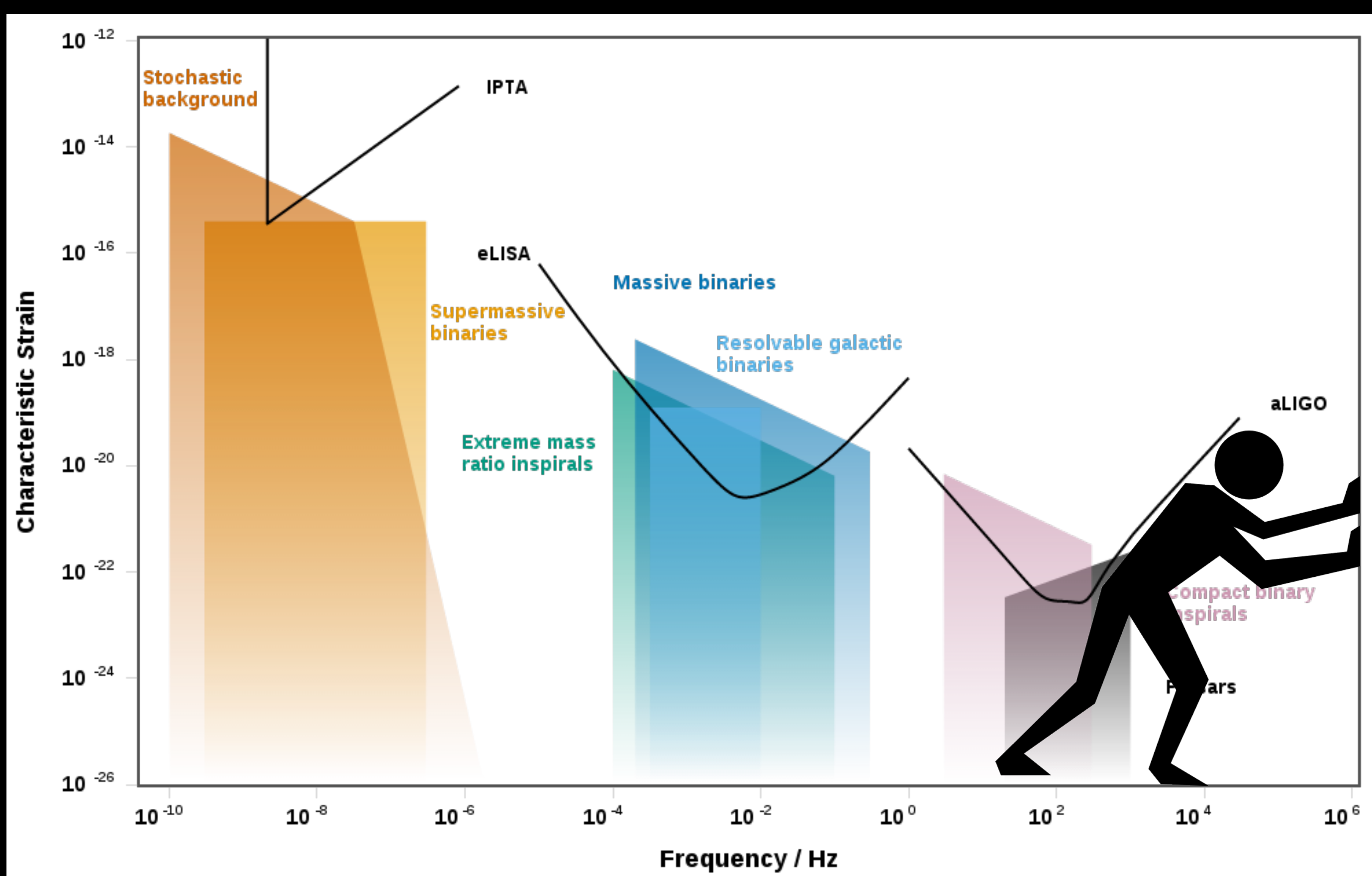

Francesco Muia

UNIVERSITY OF CAMBRIDGE

UK Research and Innovation

EPSRC

based on 2205.02153

Gabriele Franciolini

Anshuman Maharana

Advent of gravitational waves

Credits: LIGO-Virgo-KAGRA Collaborations/Frank Elavsky, Aaron Geller/Northwestern

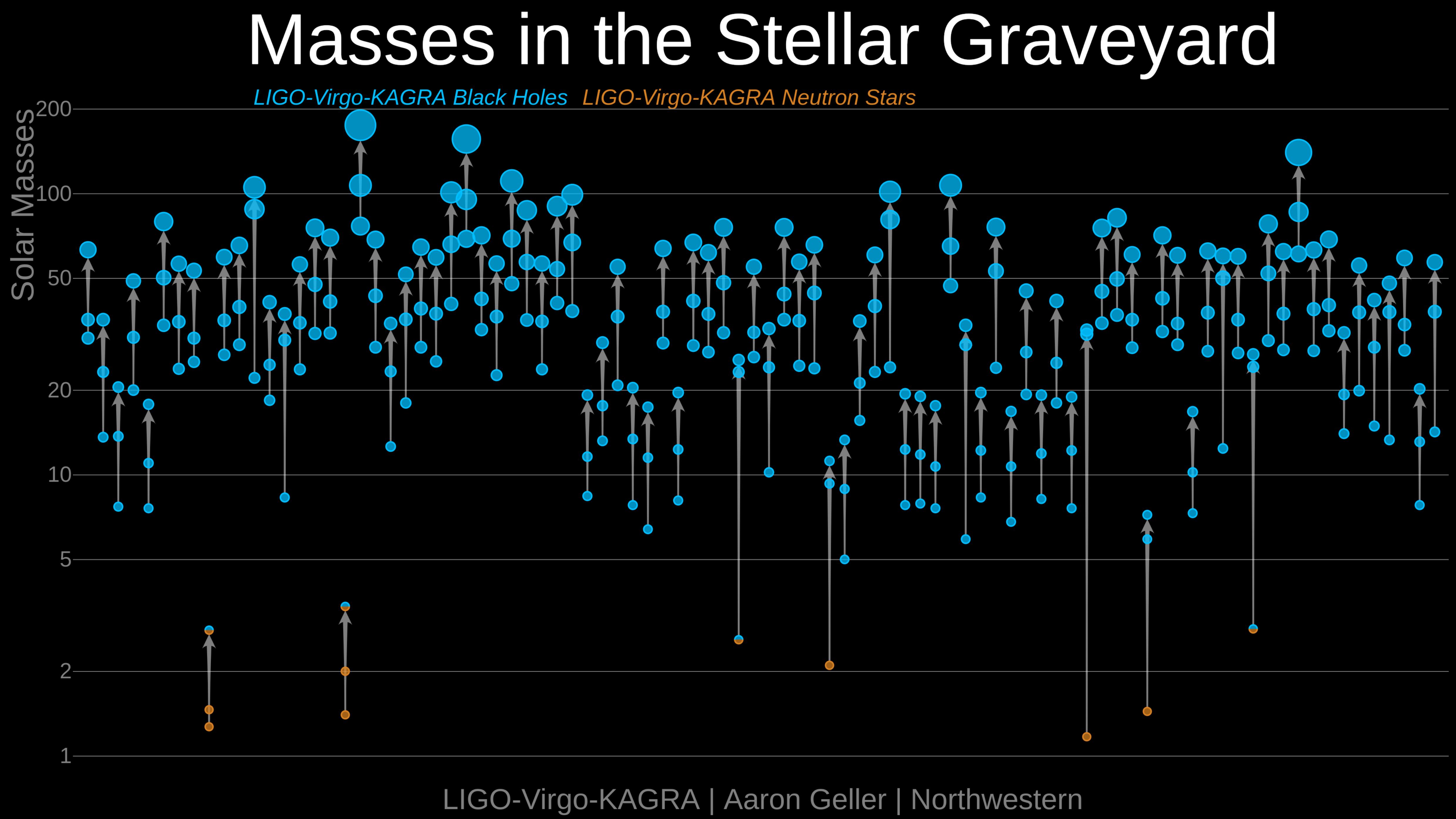

Compact object masses. Each circle represents a different compact object and the vertical scale indicates the mass as a multiple of the mass of our Sun. Blue circles represent black holes and orange circles represent neutron stars. Half-blue / half-orange mixed circles are compact objects whose classification is uncertain.

GW spectrum

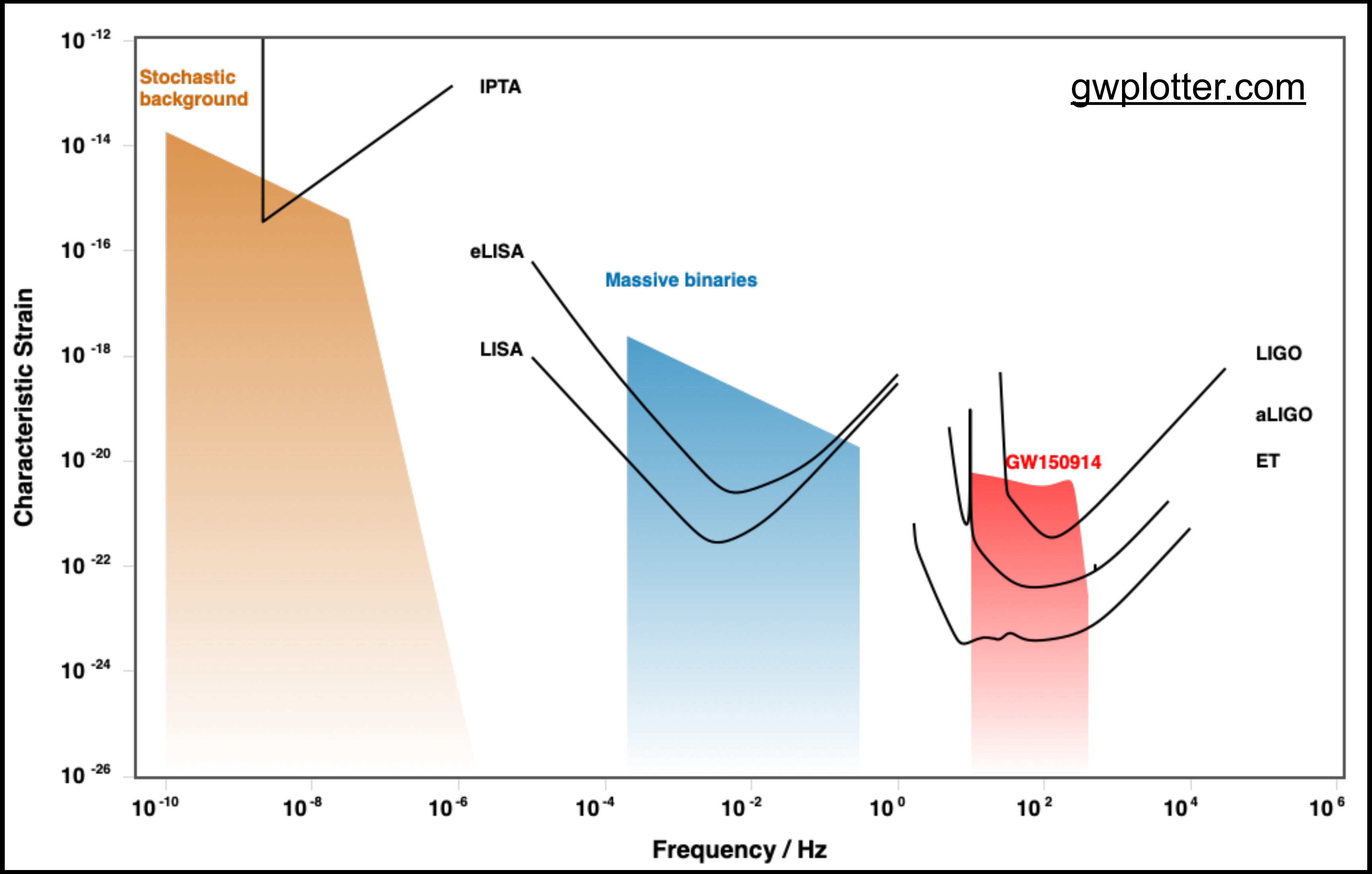

- CMB scales: inflation $(10^{-18}\,\mathrm{Hz} \lesssim f \lesssim 10^{-16}\,\mathrm{Hz})$
- PTA scales: supermassive BH mergers, cosmic strings, …
- LISA scales: galactic compact binaries, supermassive BH mergers, extreme mass ratio inspirals, phase transitions, cosmic strings, …
- LIGO scales: BH/NS binaries, phase transitions, GW bursts, …

New physics from UHF-GWs

- Natural frequency for a self-gravitating body

$$f_0 \simeq \sqrt{\frac{G\bar{\rho}}{4\pi}} \longrightarrow$$

good estimate for binary orbital frequency and pulsation frequency

New physics from UHF-GWs

- Natural frequency for a self-gravitating body

$$f_0 \simeq \sqrt{\frac{G\bar{\rho}}{4\pi}} \longrightarrow$$

good estimate for binary orbital frequency and pulsation frequency

- Astrophysical object of mass M and radius $R \geq 2GM$:

$$f_0 \lesssim 10\,\mathrm{kHz}$$

$$\downarrow$$

no astrophysical GW signal above
$f_0 \simeq 10\,\mathrm{kHz}$

cosmology

BSM physics

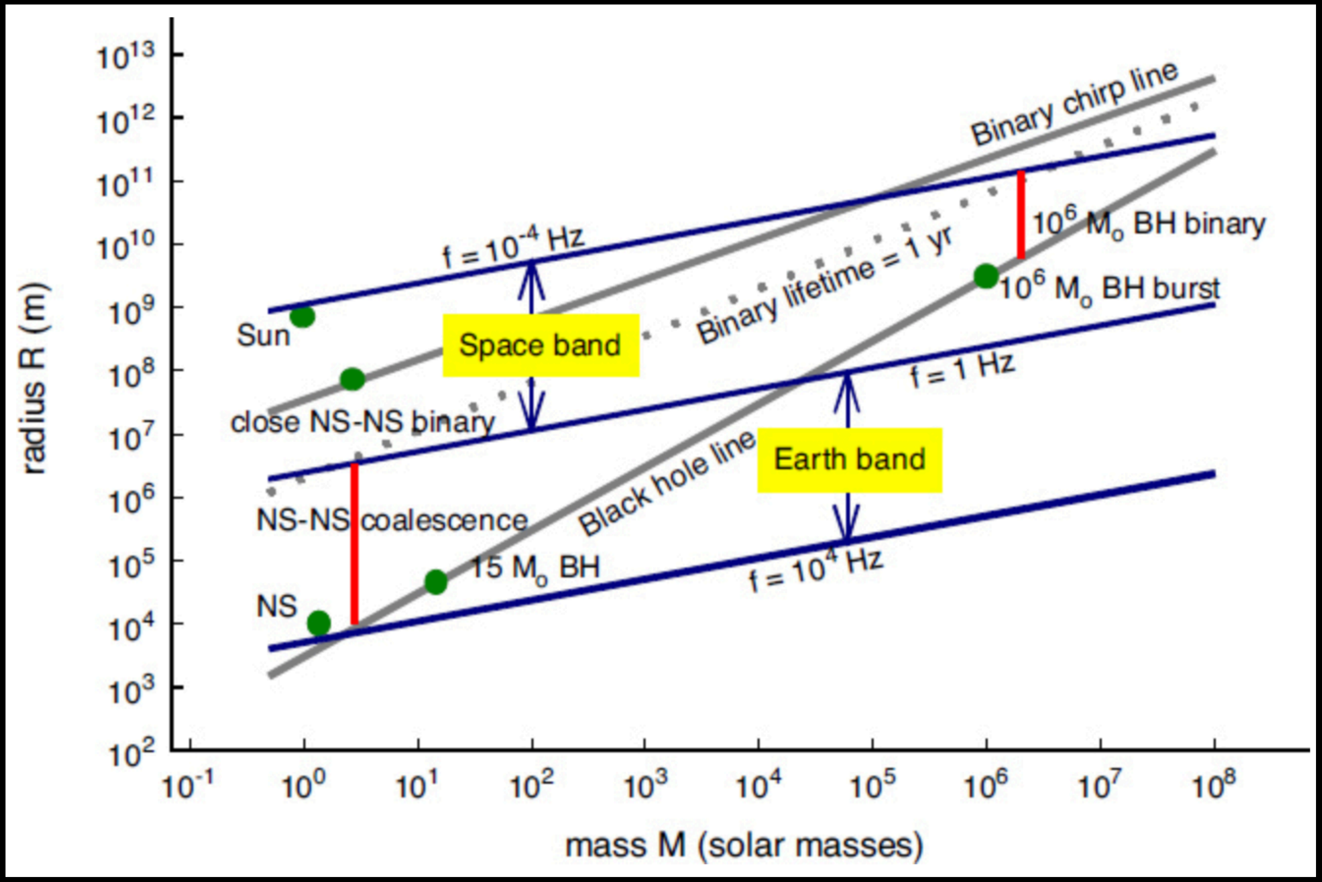

UHF-GW initiative

[Muia et al., 2020]

Challenges and Opportunities of Gravitational Wave Searches at MHz to GHz frequencies

N. Aggarwal[a], O.D. Aguiar[b], A. Bauswein[c], G. Cella[d], S. Clesse[e], A.M. Cruise[f], V. Domcke[g,*], D. G. Figueroa[h], A. Geraci[i], M. Goryachev[j], H. Grote[k], M. Hindmarsh[l,m], F. Muia[n,*], N. Mukund[o], D. Ottaway[p,q], M. Peloso[r,s], F. Quevedo[n,*], A. Ricciardone[r,s], J. Steinlechner[t,*], S. Steinlechner[u,*], S. Sun[v], M.E. Tobar[j], F. Torrenti[z], C. Unal[x], G. White[y]

Abstract

The first direct measurement of gravitational waves by the LIGO/Virgo collaboration has opened up new avenues to explore our Universe. This white paper outlines the challenges and gains expected in gravitational wave searches at frequencies above the LIGO/Virgo band, with a particular focus on the MHz and GHz range.

UHF-GW initiative

[Muia et al., 2020]

Challenges and Opportunities of Gravitational Wave Searches at MHz to GHz frequencies

N. Aggarwal[a], O.D. Aguiar[b], A. Bauswein[c], G. Cella[d], S. Clesse[e], A.M. Cruise[f], V. Domcke[g,*], D. G. Figueroa[h], A. Geraci[i], M. Goryachev[j], H. Grote[k], M. Hindmarsh[l,m], F. Muia[n,*], N. Mukund[o], D. Ottaway[p,q], M. Peloso[r,s], F. Quevedo[n,*], A. Ricciardone[r,s], J. Steinlechner[t,*], S. Steinlechner[u,*], S. Sun[v], M.E. Tobar[j], F. Torrenti[z], C. Unal[x], G. White[y]

Abstract

The first direct measurement of gravitational waves by the LIGO/Virgo collaboration has opened up new avenues to explore our Universe. This white paper outlines the challenges and gains expected in gravitational wave searches at frequencies above the LIGO/Virgo band, with a particular focus on the MHz and GHz range.

https://www.ctc.cam.ac.uk/activities/UHF-GW.php

Nancy Aggarwal

UC Davies

Valerie Domcke

CERN

Mike Cruise

University of Birmingham

Francesco Muia

University of Cambridge

Fernando Quevedo

University of Cambridge

Andreas Ringwald

DESY

Cosmological UHF-GWs

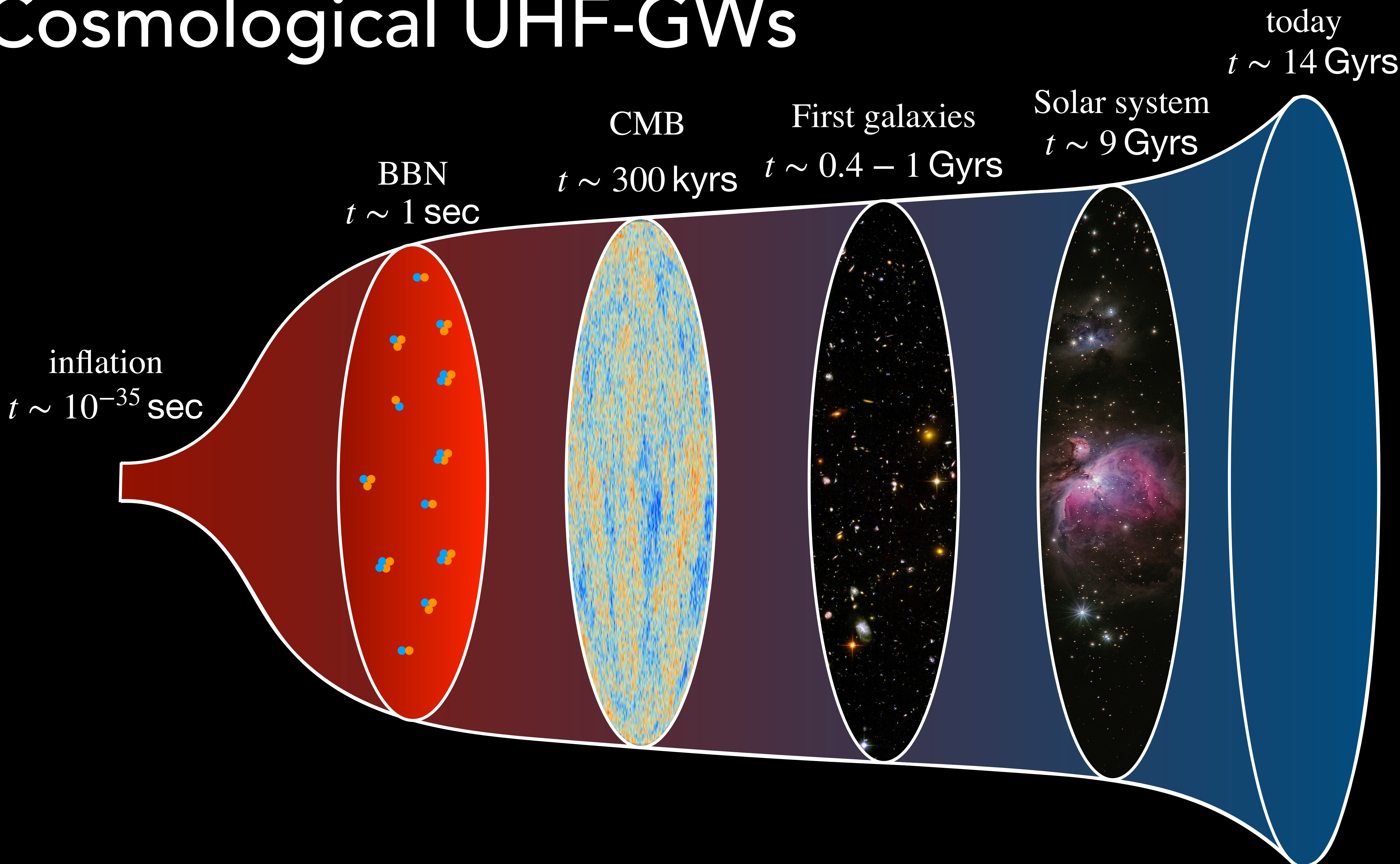

Cosmological UHF-GWs

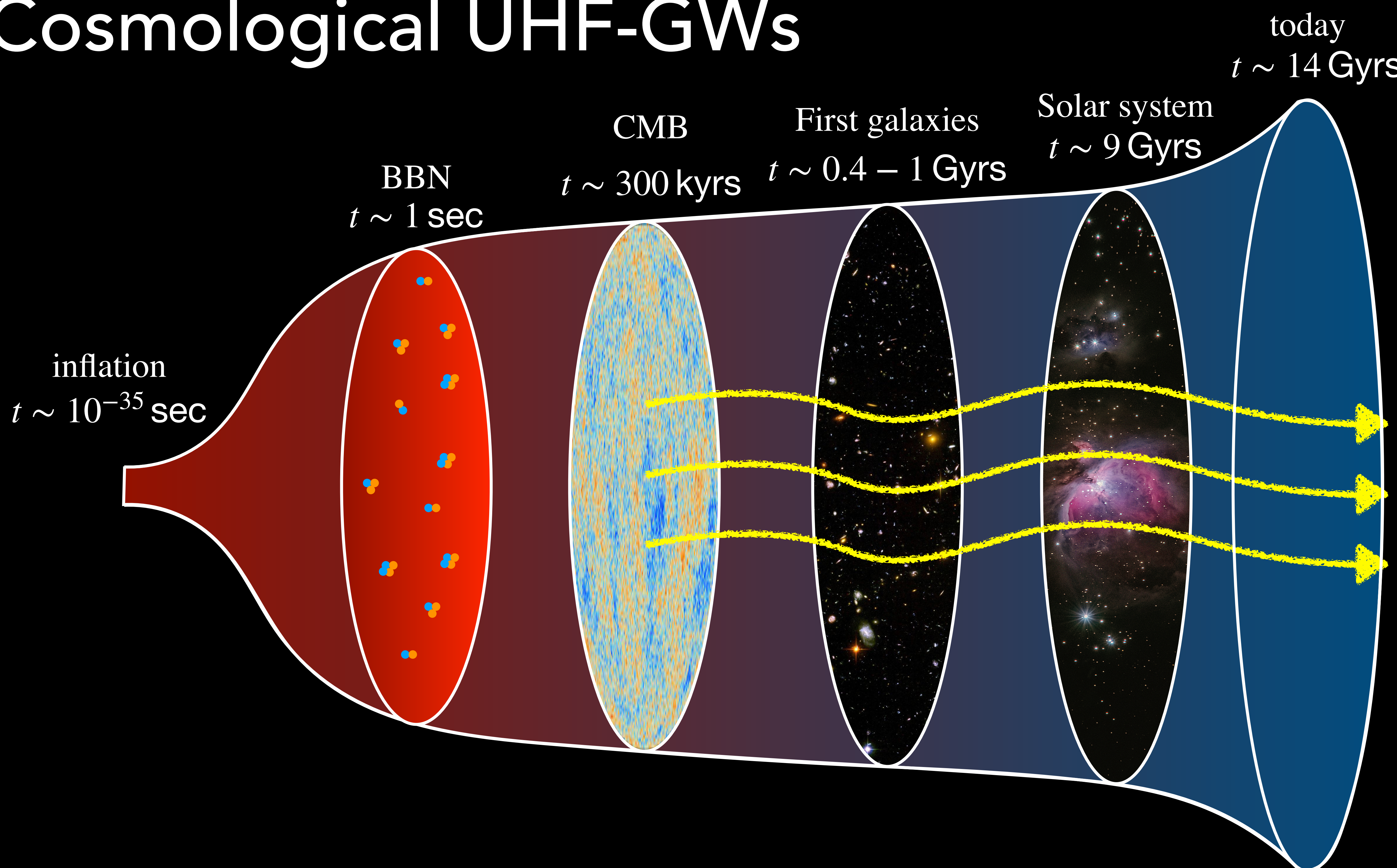

Cosmological UHF-GWs

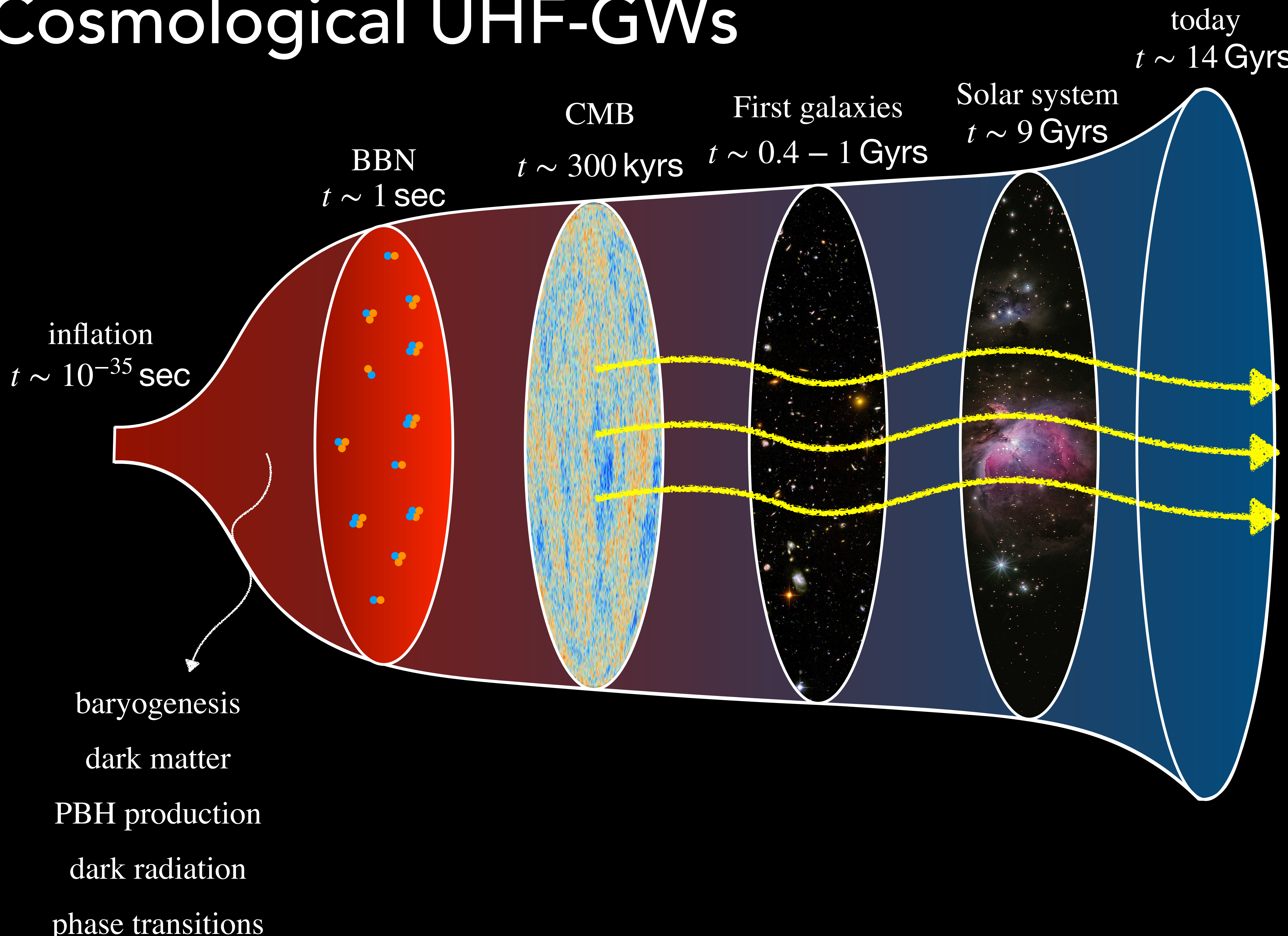

Cosmological UHF-GWs

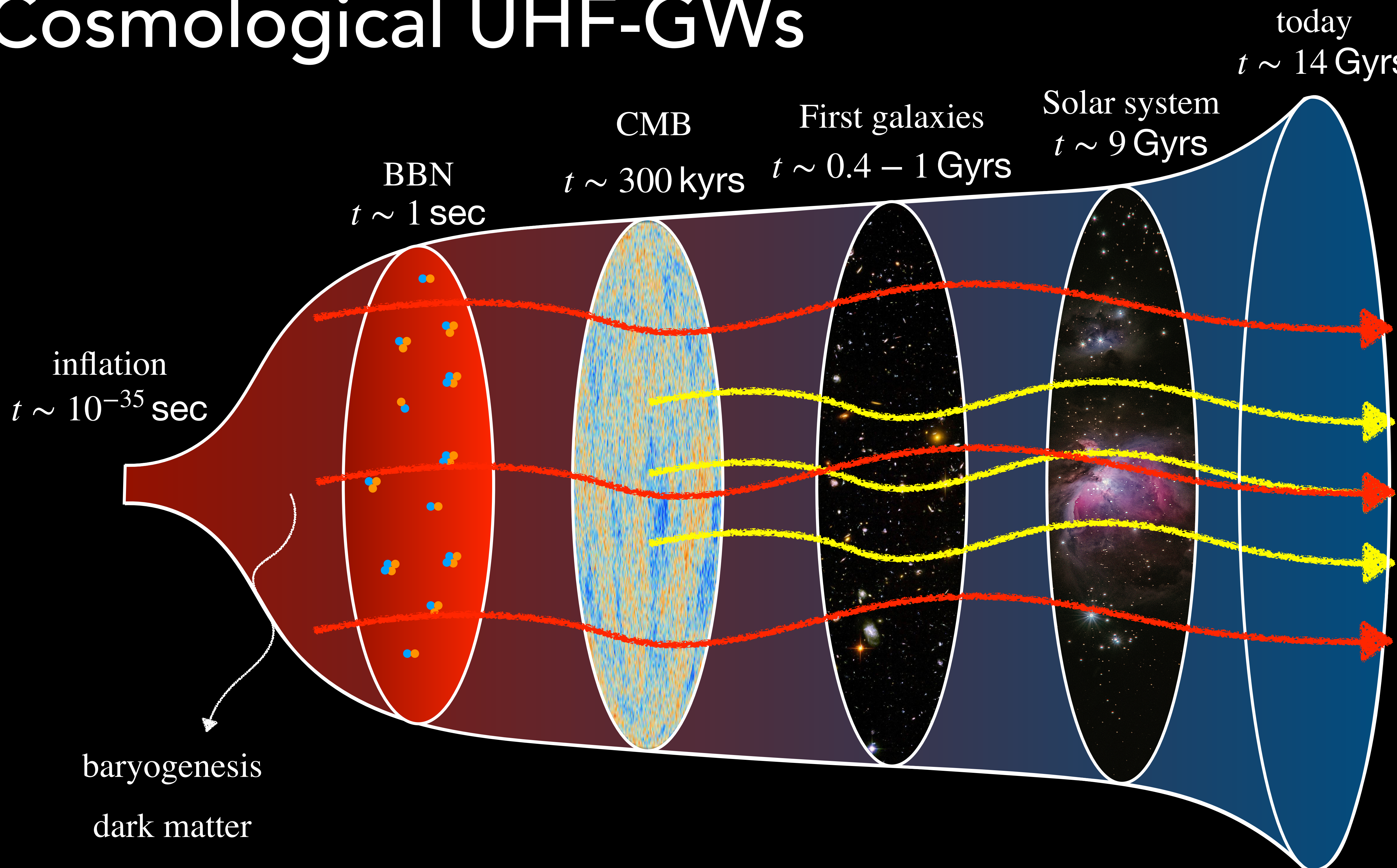

baryogenesis

dark matter

PBH production

dark radiation

phase transitions

$$\frac{\Gamma}{H} \sim \left(\frac{T}{M_p} \right)^3 \longrightarrow$$

GWs decouple immediately upon production

Cosmological signals

- Characteristic frequency $$f_0 \simeq \frac{10^{-7}}{\epsilon}\left(\frac{T_p}{\mathrm{GeV}}\right)\left(\frac{g_*(T_p)}{100}\right)^{1/6}\ \mathrm{Hz}$$

$$\epsilon = \frac{\lambda_p}{1/H_p} = \frac{\text{GW wavelength at production}}{\text{horizon size at production}} \leq 1$$ (causality)

Cosmological signals

- Characteristic frequency

$$f_0 \simeq \frac{10^{-7}}{\epsilon}\left(\frac{T_p}{\mathrm{GeV}}\right)\left(\frac{g_*(T_p)}{100}\right)^{1/6}\ \mathrm{Hz}$$

$$\epsilon = \frac{\lambda_p}{1/H_p} = \frac{\text{GW wavelength at production}}{\text{horizon size at production}} \leq 1 \qquad \text{(causality)}$$

For $\epsilon \sim 1$

detection	production time	production T
10^{-5} Hz	10^{-11} sec	100 GeV
0.16 Hz	10^{-19} sec	10^{6} GeV
1.6 kHz	10^{-27} sec	10^{9} GeV
1.6 MHz	10^{-33} sec	10^{13} GeV
1.6 GHz	10^{-39} sec	10^{16} GeV

beyond LIGO

~GUT/string scale

Cosmological signals

- Characteristic frequency $$f_0 \simeq \frac{10^{-7}}{\epsilon}\left(\frac{T_p}{\mathrm{GeV}}\right)\left(\frac{g_*(T_p)}{100}\right)^{1/6}\ \mathrm{Hz}$$

$$\epsilon = \frac{\lambda_p}{1/H_p} = \frac{\text{GW wavelength at production}}{\text{horizon size at production}} \leq 1 \qquad \text{(causality)}$$

For $\epsilon \sim 1$

detection	production time	production T
10^{-5} Hz	10^{-11} sec	100 GeV
0.16 Hz	10^{-19} sec	10^{6} GeV
1.6 kHz	10^{-27} sec	10^{9} GeV
1.6 MHz	10^{-33} sec	10^{13} GeV
1.6 GHz	10^{-39} sec	10^{16} GeV

beyond LIGO

~GUT/string scale

- Stochastic signal: superposition of independent signals emitted by a huge number of uncorrelated regions
  - Homogeneous and isotropic
  - Unpolarized
  - Gaussian

Amplitude of cosmological signals

$$h_c \simeq 1.3 \times 10^{-21} \left(\frac{1\,\mathrm{kHz}}{f} \right) \sqrt{h_0^2 \Omega_{\mathrm{gw}}(f)}$$

BBN bound $\quad h_c \lesssim 3 \times 10^{-24} \left(\frac{1\,\mathrm{kHz}}{f} \right)$

$$h_0^2\, \Omega_{\mathrm{gw}}^{\mathrm{BBN}} \sim 10^{-6}$$

f_0	h_c
10^2 Hz	3×10^{-23}
MHz	3×10^{-27}
GHz	3×10^{-30}

[Muia et al., 2020]

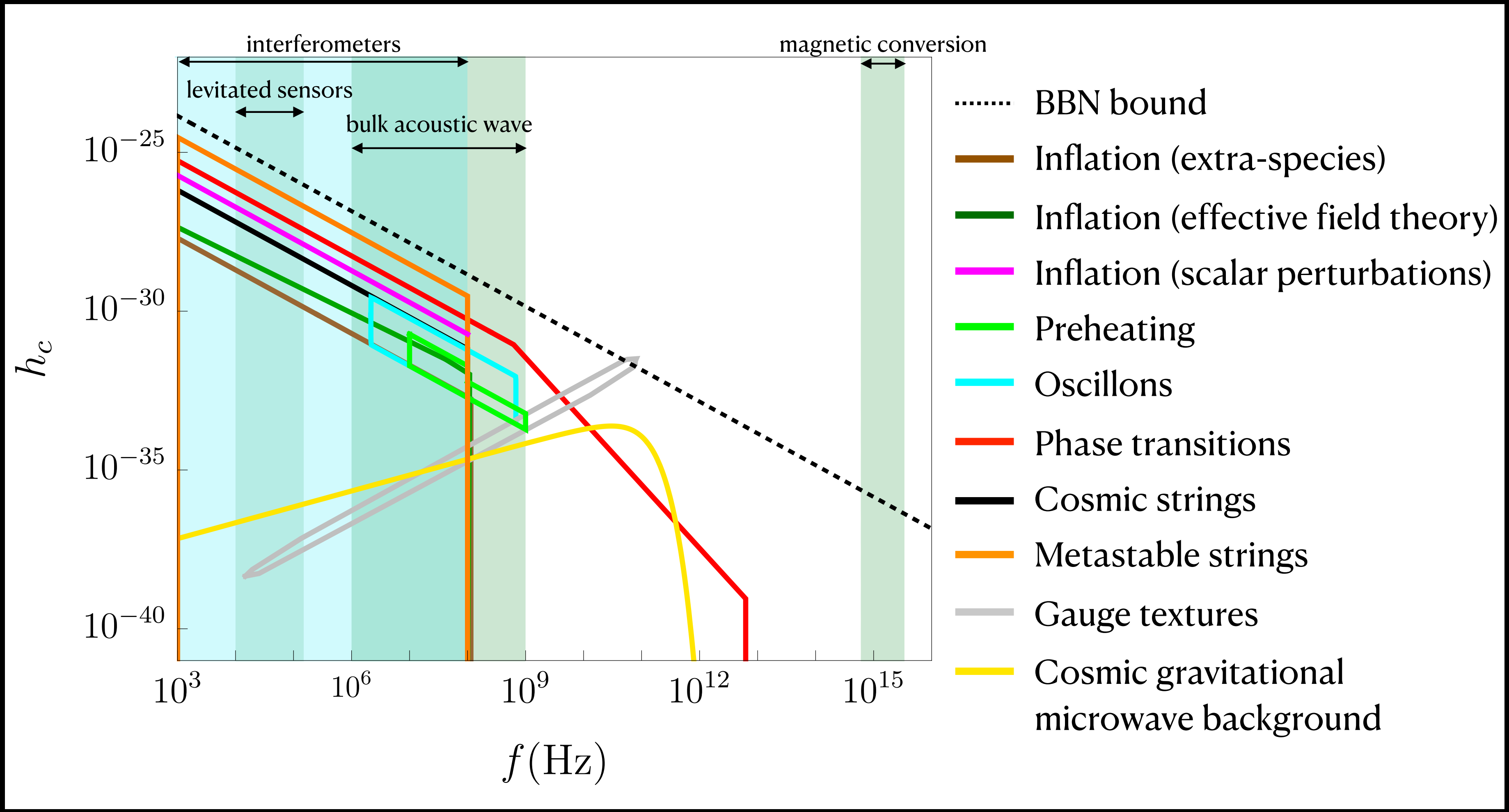

Late Universe

[Muia et al., 2020]

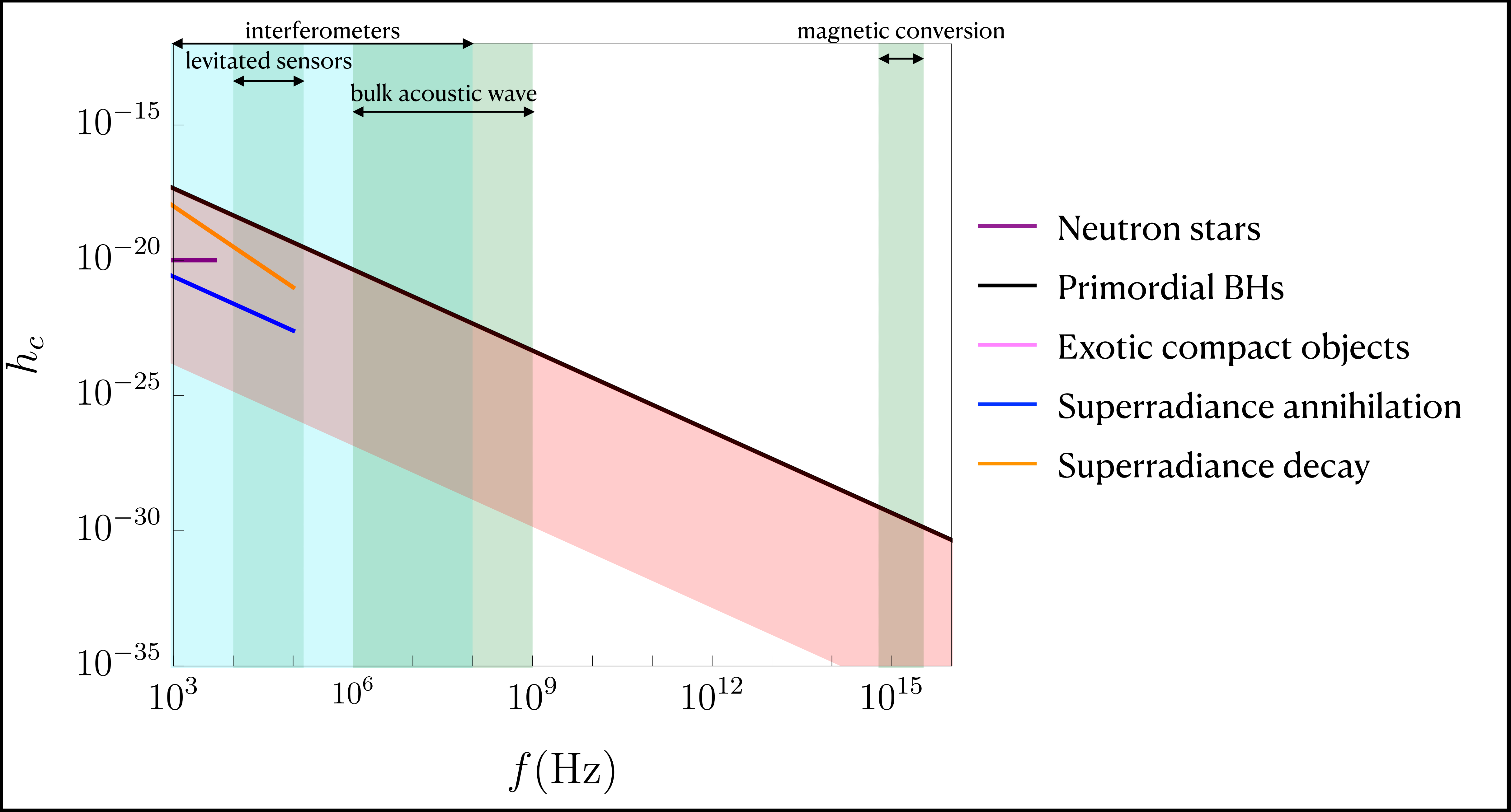

General properties

- Coherent signals are possible
- Strain: $h_c \lesssim 10^{-20}$
- Frequency: $f \gtrsim 10\,\mathrm{kHz}$ ↔ BSM physics

Benchmark distance: 10 kpc

↓

is this reasonable?

Primordial black holes

For a comprehensive list of references and an exceptional introduction to PBHs, please check G. Franciolini PhD thesis

$$f_{\rm ISCO} \simeq 4.4 \times 10^3\,{\rm Hz}\left(\frac{M_\odot}{m_1+m_2}\right)$$

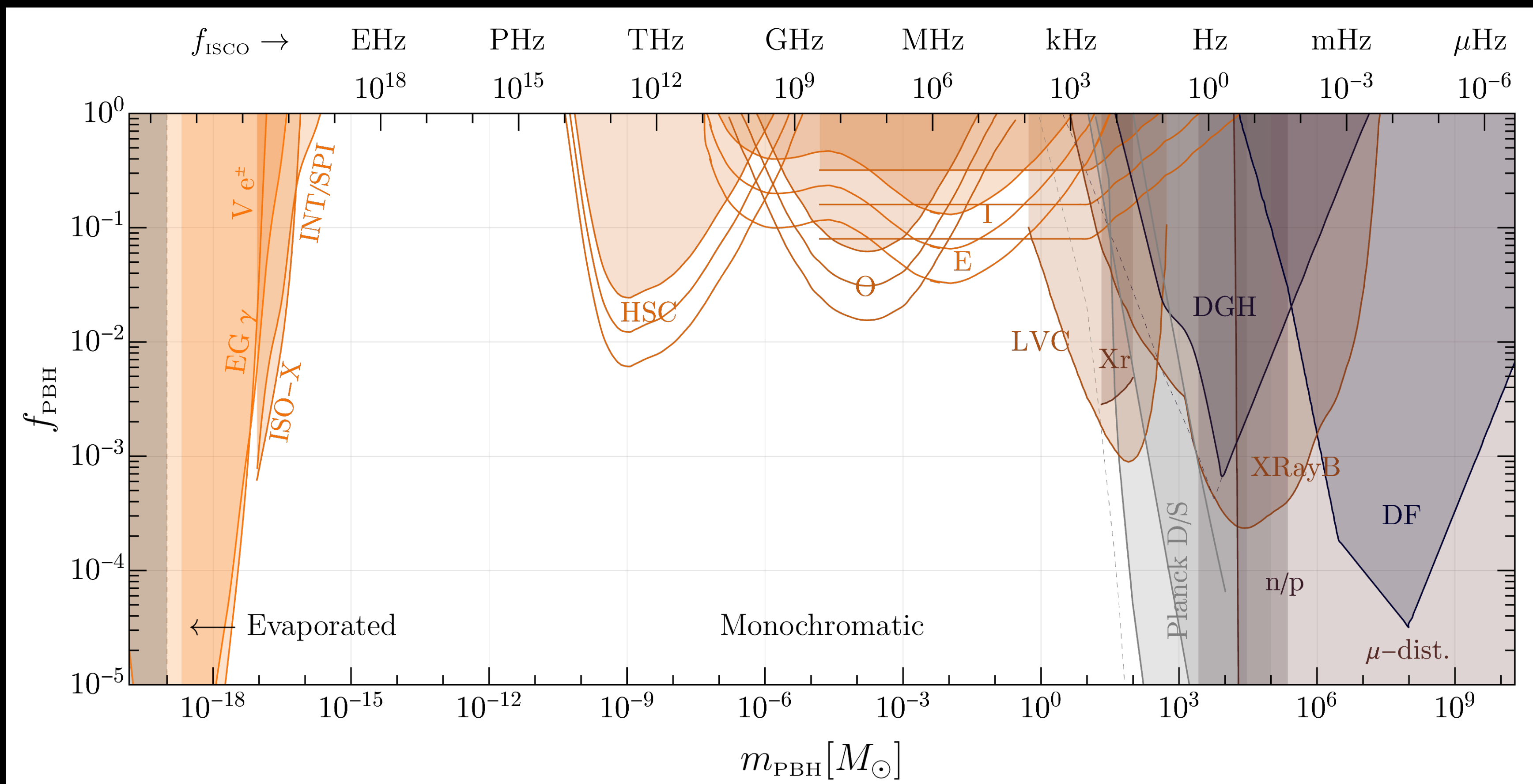

Constraints

EG γ, V $e^{\pm}$, INT/SPI, ISO-X: evaporation

HSC, EROS, OGLE, Icarus: lensing

LVC: gravitational waves

Xr, XRayB: X-rays observations

Planck D/S, μ-dist.: CMB distortions

DGH: Dwarf Galaxy heating

DF: dynamical friction

n/p: neutron to proton ratio

[Carr et al., 2020]

Primordial black holes

For a comprehensive list of references and an exceptional introduction to PBHs, please check G. Franciolini PhD thesis

$$f_{\mathrm{ISCO}} \simeq 4.4 \times 10^3\,\mathrm{Hz}\left(\frac{M_\odot}{m_1+m_2}\right)$$

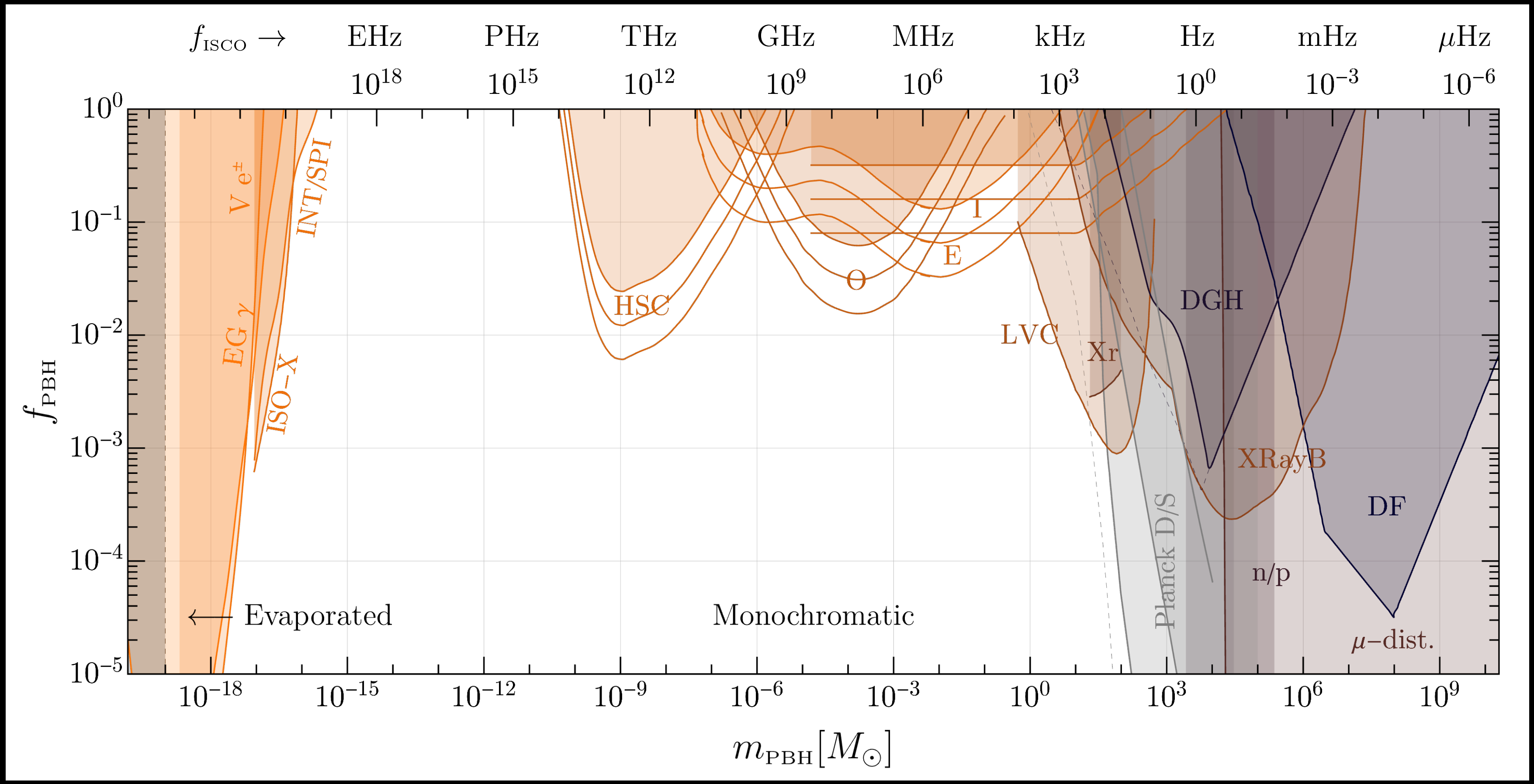

Constraints

EG γ, V $e^\pm$, INT/SPI, ISO-X: evaporation

HSC, EROS, OGLE, Icarus: lensing

LVC: gravitational waves

Xr, XRayB: X-rays observations

Planck D/S, μ-dist.: CMB distortions

DGH: Dwarf Galaxy heating

DF: dynamical friction

n/p: neutron to proton ratio

[Carr et al., 2020]

$$f_{\mathrm{PBH}}(M) \equiv \frac{\Omega_{\mathrm{PBH}}(M)}{\Omega_{\mathrm{DM}}}$$

$$f_{\mathrm{tot}} = \frac{\Omega_{\mathrm{PBH}}}{\Omega_{\mathrm{DM}}} = \int \frac{dM}{2M}\, f_{\mathrm{PBH}}(M)$$

only region that still admits 100% of dark matter in PBHs is $(10^{-16} - 10^{-11})\,M_\odot$

all constraints are derived under specific assumptions

Primordial black holes

For a comprehensive list of references and an exceptional introduction to PBHs, please check G. Franciolini PhD thesis

$$f_{\rm ISCO} \simeq 4.4 \times 10^3\,{\rm Hz} \left(\frac{M_\odot}{m_1 + m_2}\right)$$

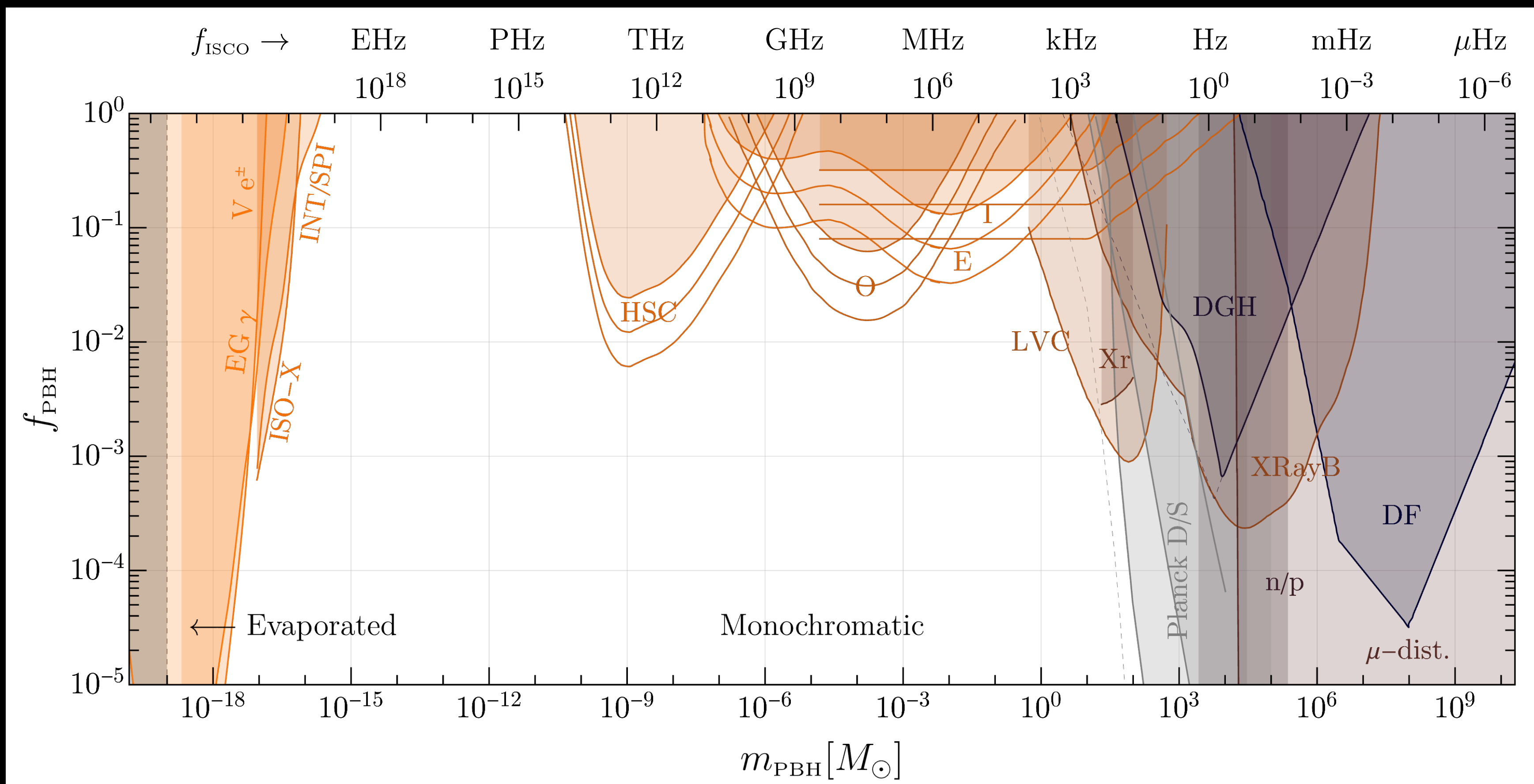

Constraints

EG γ, V $e^\pm$, INT/SPI, ISO-X: evaporation

HSC, EROS, OGLE, Icarus: lensing

LVC: gravitational waves

Xr, XRayB: X-rays observations

Planck D/S, μ-dist.: CMB distortions

DGH: Dwarf Galaxy heating

DF: dynamical friction

n/p: neutron to proton ratio

[Carr et al., 2020]

$$f_{\rm PBH}(M) \equiv \frac{\Omega_{\rm PBH}(M)}{\Omega_{\rm DM}}$$

$$f_{\rm tot} = \frac{\Omega_{\rm PBH}}{\Omega_{\rm DM}} = \int \frac{dM}{2M}\, f_{\rm PBH}(M)$$

only region that still admits 100% of dark matter in PBHs is $(10^{-16} - 10^{-11})\,M_\odot$

all constraints are derived under specific assumptions $\longrightarrow$ important to provide complementary and independent probes

Primordial black holes

- A PBH is formed when a mode re-enter the horizon if the related density perturbation is above a certain threshold

Image taken from G. Franciolini PhD thesis

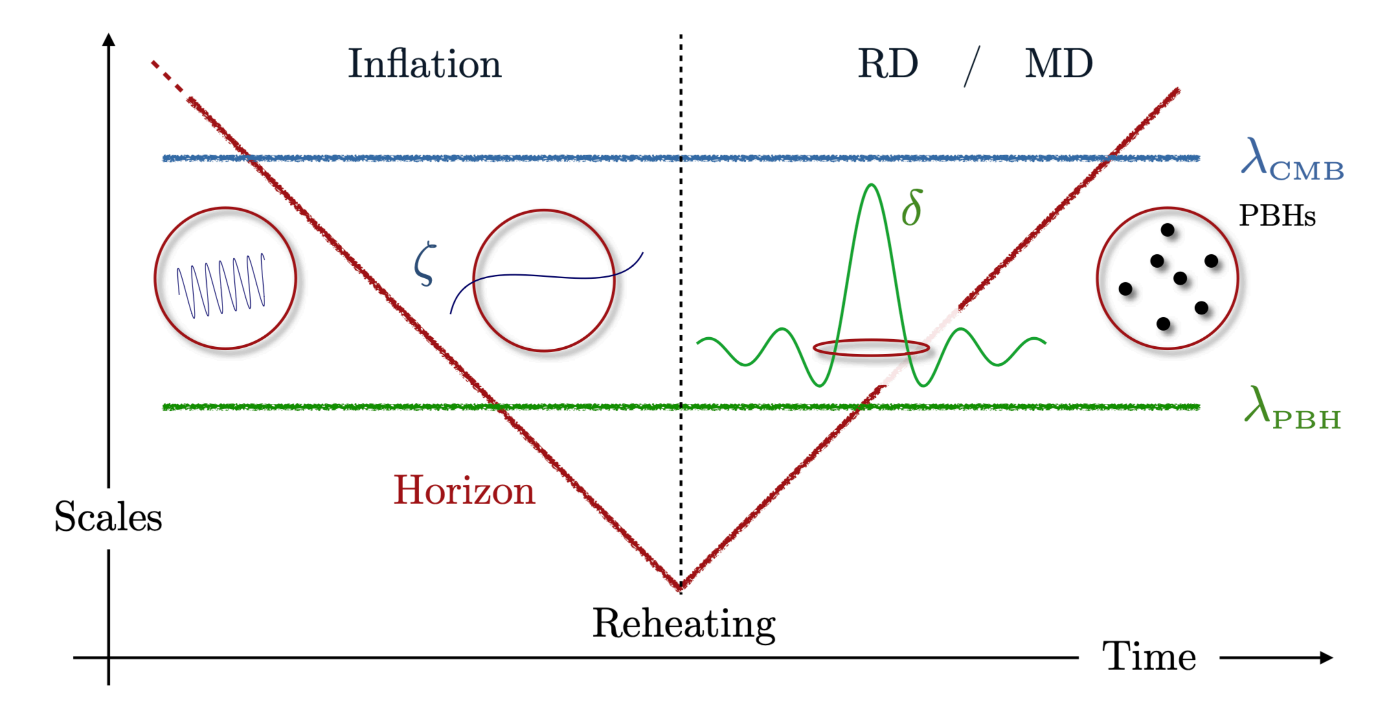

Primordial black holes

- A PBH is formed when a mode re-enter the horizon if the related density perturbation is above a certain threshold

Image taken from G. Franciolini PhD thesis

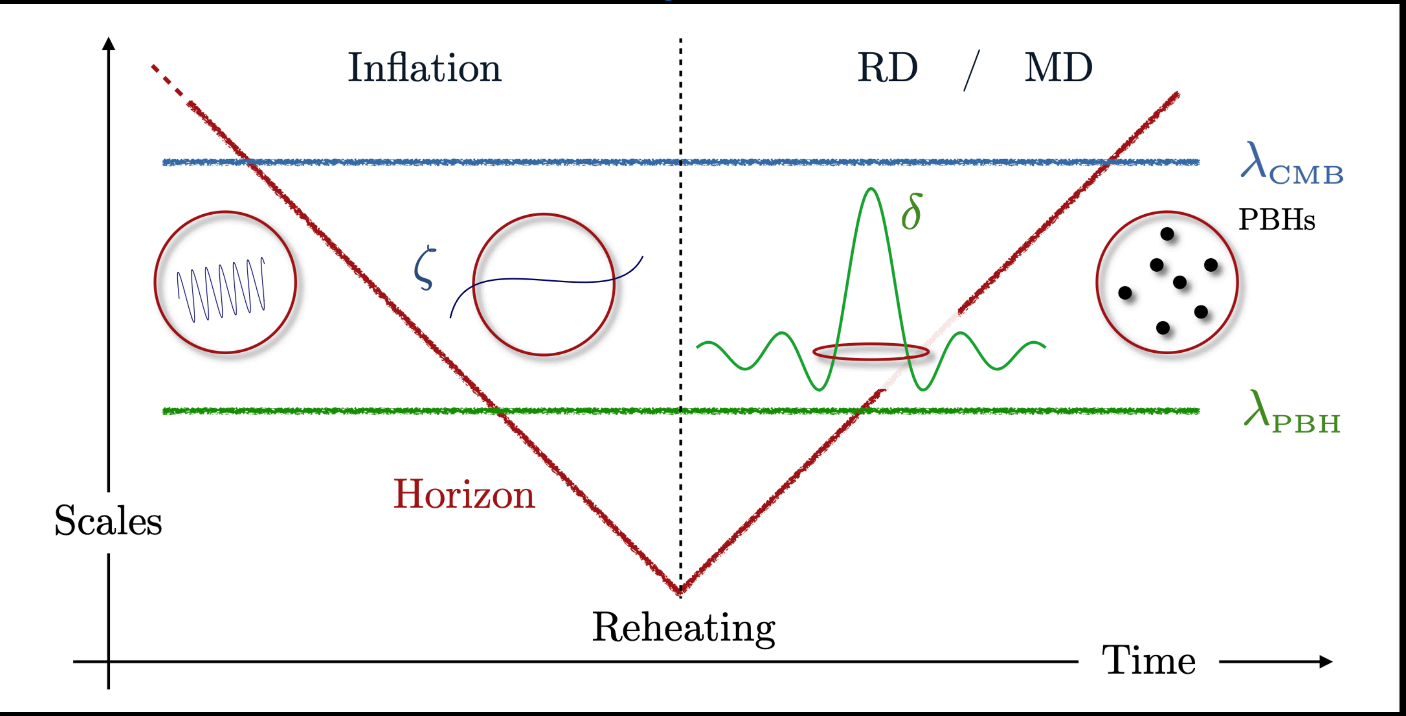

hydrodynamical simulations give

$$\frac{\delta\rho}{\rho} \gtrsim 0.3$$

[Nadezhin et al., '74]
[Niemeyer et al., '99]
[Shibata et al., '99]
[Musco et al., '05]

Primordial black holes

- A PBH is formed when a mode re-enter the horizon if the related density perturbation is above a certain threshold

Image taken from G. Franciolini PhD thesis

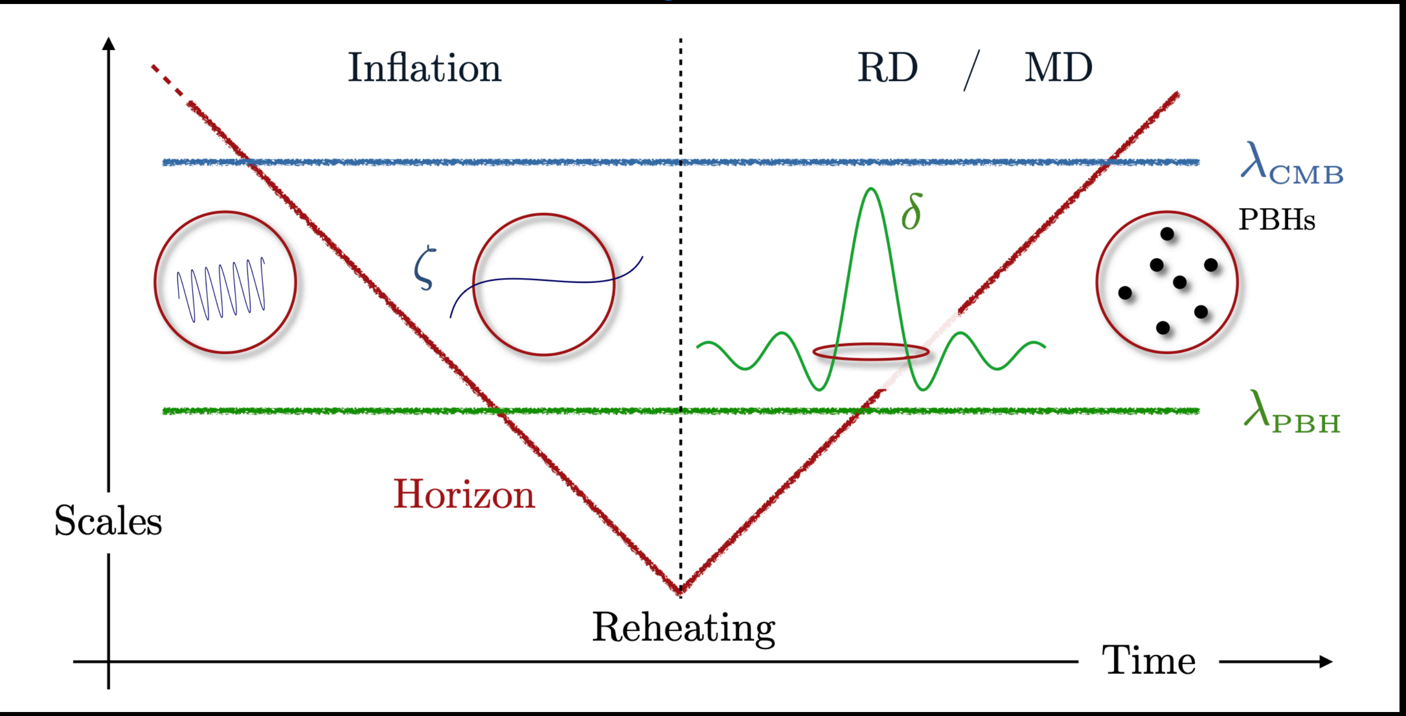

hydrodynamical simulations give

$$\frac{\delta\rho}{\rho} \gtrsim 0.3$$

[Nadezhin et al., '74]
[Niemeyer et al., '99]
[Shibata et al., '99]
[Musco et al., '05]

- The PBH mass is determined by the amount of energy contained in a horizon patch at formation

$$M \sim \frac{c^3 t}{G} \sim 10^{15} \left(\frac{t}{10^{-23}\,\mathrm{sec}}\right) \mathrm{g}$$

Primordial black holes

- A PBH is formed when a mode re-enter the horizon if the related density perturbation is above a certain threshold

Image taken from G. Franciolini PhD thesis

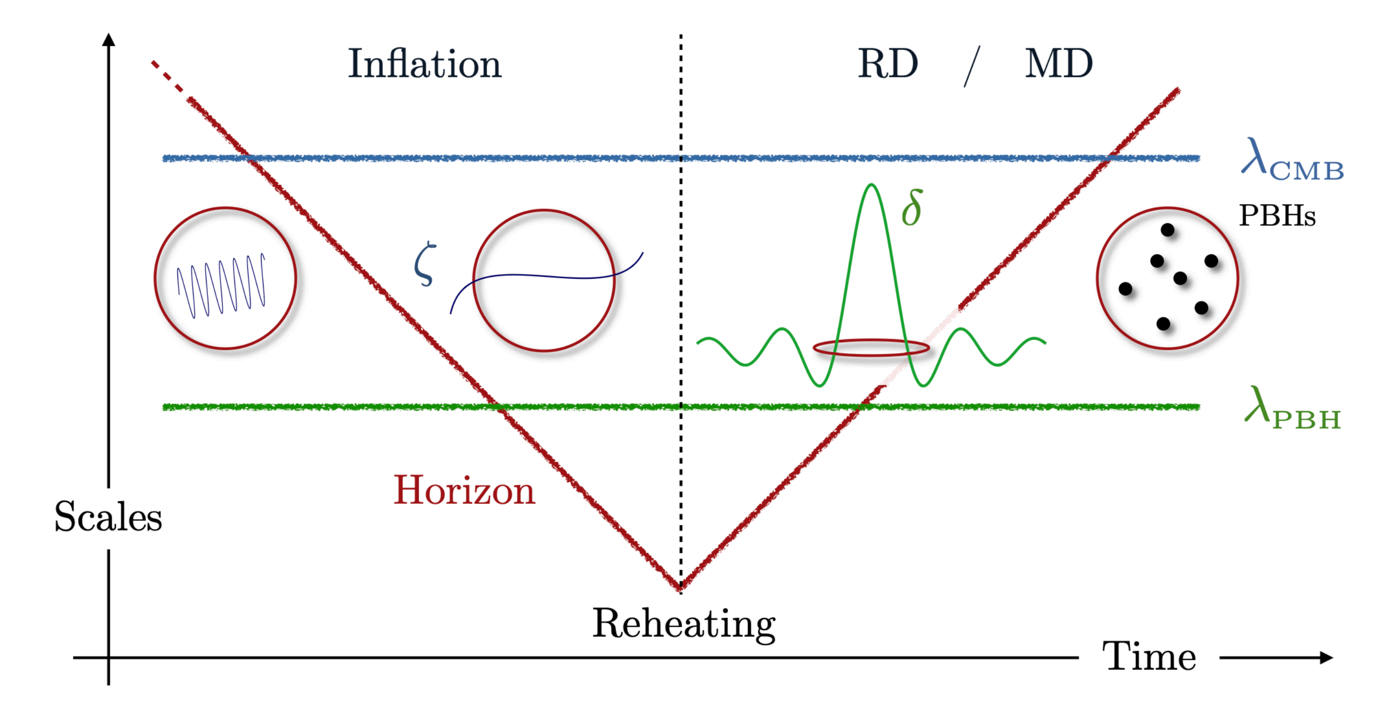

hydrodynamical simulations give

$$\frac{\delta\rho}{\rho} \gtrsim 0.3$$

[Nadezhin et al., '74]
[Niemeyer et al., '99]
[Shibata et al., '99]
[Musco et al., '05]

- The PBH mass is determined by the amount of energy contained in a horizon patch at formation

$$M \sim \frac{c^3 t}{G} \sim 10^{15} \left(\frac{t}{10^{-23}\,\mathrm{sec}}\right) \mathrm{g}$$

- PBHs evaporate through Hawking radiation

$$\tau = \frac{10240\pi}{N_{\mathrm{eff}}^{\mathrm{evap}}} \frac{m_{\mathrm{PBH}}^3}{m_{\mathrm{p}}^4} \simeq 10\,\mathrm{Gyr} \left(\frac{N_{\mathrm{eff}}^{\mathrm{evap}}}{100}\right)^{-1} \left(\frac{m_{\mathrm{PBH}}}{3\times 10^{-19}\,M_\odot}\right)^3 \longrightarrow$$

can be DM for $M \gtrsim 10^{-18}\,M_\odot$

PBH binary formation and evolution

We adopt state-of-the art models for PBH binary formation and evolution

[Raidal et al., 2018]

[Ali-Haımoud et al., 2017]

PBH binary formation and evolution

We adopt state-of-the art models for PBH binary formation and evolution
[Raidal et al., 2018]
[Ali-Haımoud et al., 2017]

- Standard formation scenario: collapse during radiation domination of Gaussian perturbations imprinted during the inflationary era.

PBH binary formation and evolution

We adopt state-of-the art models for PBH binary formation and evolution

[Raidal et al., 2018]
[Ali-Haımoud et al., 2017]

- Standard formation scenario: collapse during radiation domination of Gaussian perturbations imprinted during the inflationary era.

→ PBHs are expected to follow a Poisson spatial distribution at formation

→ a pair of PBHs decouple from Hubble expansion when gravitational attraction starts dominating over Hubble flow

[Nakamura et al., 1997]
[Yoka et al., 1998]

PBH binary formation and evolution

We adopt state-of-the art models for PBH binary formation and evolution

[Raidal et al., 2018]

[Ali-Haımoud et al., 2017]

- Standard formation scenario: collapse during radiation domination of Gaussian perturbations imprinted during the inflationary era.

→ PBHs are expected to follow a Poisson spatial distribution at formation

→ a pair of PBHs decouple from Hubble expansion when gravitational attraction starts dominating over Hubble flow

[Nakamura et al., 1997]

[Yoka et al., 1998]

→ Initially, radial motion

→ Acquires angular momentum due to tidal torques from surrounding overdensities

→ Shrinks due to loss of energy due to GW emission

PBH binary formation and evolution

We adopt state-of-the art models for PBH binary formation and evolution
[Raidal et al., 2018]
[Ali-Haımoud et al., 2017]

- Standard formation scenario: collapse during radiation domination of Gaussian perturbations imprinted during the inflationary era.

$\longrightarrow$ PBHs are expected to follow a Poisson spatial distribution at formation

$\longrightarrow$ a pair of PBHs decouple from Hubble expansion when gravitational attraction starts dominating over Hubble flow
[Nakamura et al., 1997]
[Yoka et al., 1998]

$\longrightarrow$ Initially, radial motion

$\longrightarrow$ Acquires angular momentum due to tidal torques from surrounding overdensities

$\longrightarrow$ Shrinks due to loss of energy due to GW emission

- Merger rate at time t:

$$\psi(M) = \frac{1}{\rho_{\rm PBH}} \frac{d\rho_{\rm PBH}(M)}{dM}$$

PBH mass distribution

$$\frac{d^2 R_{\rm PBH}}{dm^2} = \frac{7.5\times 10^{-2}}{\mathrm{kpc}^3 \times \mathrm{yr}} f_{\rm PBH}^{\frac{53}{57}} \left(\frac{t}{t_0}\right)^{-\frac{34}{37}} \left(\frac{M_{\rm tot}}{10^{-12}\,M_\odot}\right)^{-\frac{32}{37}} \left(\frac{m}{M_{\rm tot}}\right)^{-1.84} S(M_{\rm tot}, f_{\rm PBH}, \psi)\ \psi^2(m)$$

[Raidal et al., 2018]

$\hookrightarrow$ suppression factor

PBH binary formation and evolution

We adopt state-of-the art models for PBH binary formation and evolution
[Raidal et al., 2018]
[Ali-Haımoud et al., 2017]

- Standard formation scenario: collapse during radiation domination of Gaussian perturbations imprinted during the inflationary era.

$\longrightarrow$ PBHs are expected to follow a Poisson spatial distribution at formation

$\longrightarrow$ a pair of PBHs decouple from Hubble expansion when gravitational attraction starts dominating over Hubble flow
[Nakamura et al., 1997]
[Yoka et al., 1998]

$\longrightarrow$ Initially, radial motion

$\longrightarrow$ Acquires angular momentum due to tidal torques from surrounding overdensities

$\longrightarrow$ Shrinks due to loss of energy due to GW emission

- Merger rate at time t:

$$\psi(M) = \frac{1}{\rho_{\rm PBH}} \frac{d\rho_{\rm PBH}(M)}{dM}$$

PBH mass distribution

$$\frac{d^2 R_{\rm PBH}}{dm^2} = \frac{7.5 \times 10^{-2}}{\mathrm{kpc}^3 \times \mathrm{yr}} f_{\rm PBH}^{\frac{53}{57}} \left(\frac{t}{t_0}\right)^{-\frac{34}{37}} \left(\frac{M_{\rm tot}}{10^{-12}\, M_\odot}\right)^{-\frac{32}{37}} \left(\frac{m}{M_{\rm tot}}\right)^{-1.84} S(M_{\rm tot}, f_{\rm PBH}, \psi)\ \psi^2(m)$$

[Raidal et al., 2018]

$\longrightarrow$ suppression factor

$$S \equiv S_1 \times S_2$$

S_1: interactions at formation epoch between binary and DM inhomogeneities

[Hutsi et al., 2021]

S_2: effect of successive disruption of binaries that populate PBH clusters

PBH binary formation and evolution

- Late-time dynamical capture: PBH binary formation is induced by GW capture in the present age dense DM environments

  [Bird et al., 2016]
  [Quinlan et al., 1989]

  → subdominant with respect to early universe formation

  → increasingly less relevant for light PBHs

$$\frac{R_{\mathrm{PBH}}^{\mathrm{cap}}}{R_{\mathrm{PBH}}} \sim m_{\mathrm{PBH}}^{\frac{265}{777}}$$

PBH binary formation and evolution

- Late-time dynamical capture: PBH binary formation is induced by GW capture in the present age dense DM environments
  [Bird et al., 2016]
  [Quinlan et al., 1989]
  → subdominant with respect to early universe formation
  → increasingly less relevant for light PBHs

$$\frac{R_{\rm PBH}^{\rm cap}}{R_{\rm PBH}} \sim m_{\rm PBH}^{\frac{265}{777}}$$

- Accretion could affect individual masses, spins and the binary's orbital geometry
  ⟶ on light PBH binaries is irrelevant and cannot affect the merger rate

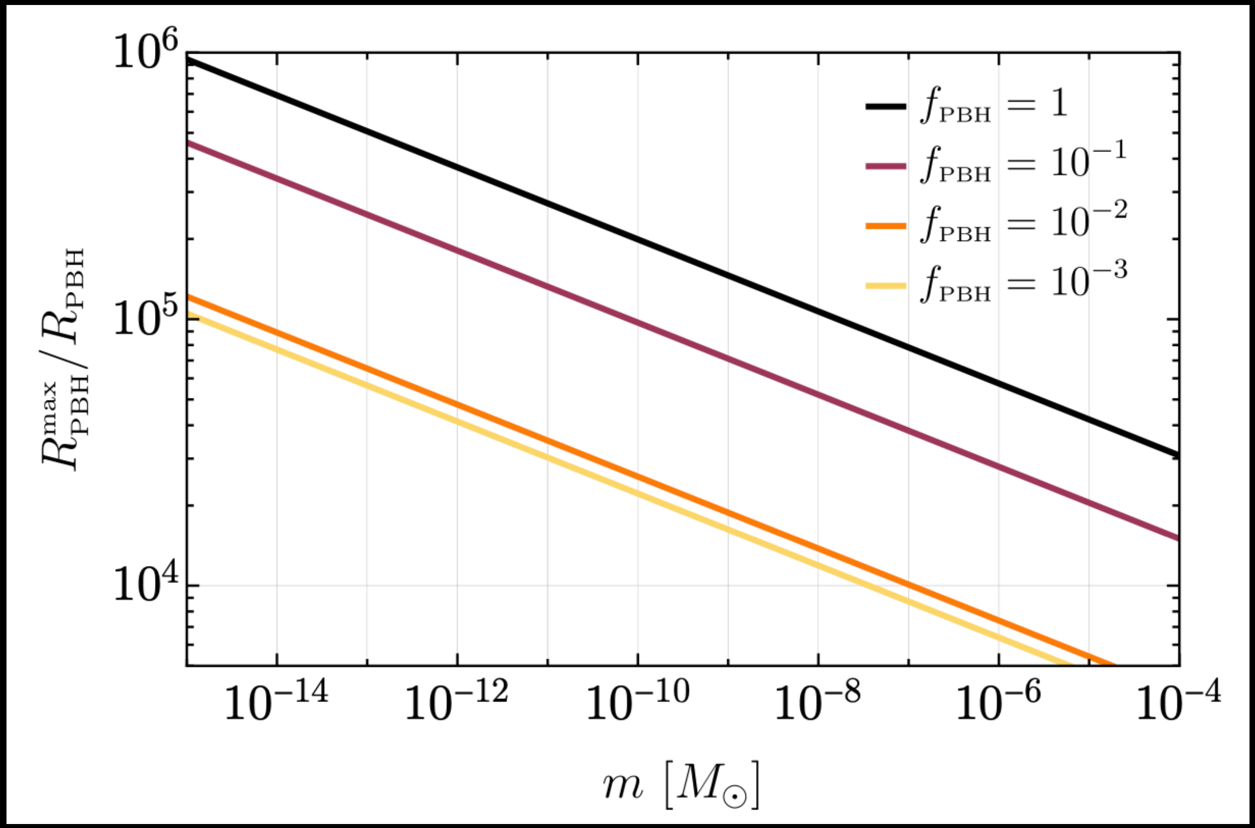

PBH binary formation and evolution

- Late-time dynamical capture: PBH binary formation is induced by GW capture in the present age dense DM environments
  [Bird et al., 2016]
  [Quinlan et al., 1989]

  $\longrightarrow$ subdominant with respect to early universe formation

  $\longrightarrow$ increasingly less relevant for light PBHs

$$\frac{R^{\rm cap}_{\rm PBH}}{R_{\rm PBH}} \sim m_{\rm PBH}^{\frac{265}{777}}$$

- Accretion could affect individual masses, spins and the binary's orbital geometry

  $\longrightarrow$ on light PBH binaries is irrelevant and cannot affect the merger rate

- Clustering at formation due to local non-Gaussianities of primordial perturbations
  [De Luca et al., 2021]

  $\downarrow$

  maximum theoretical merger rate

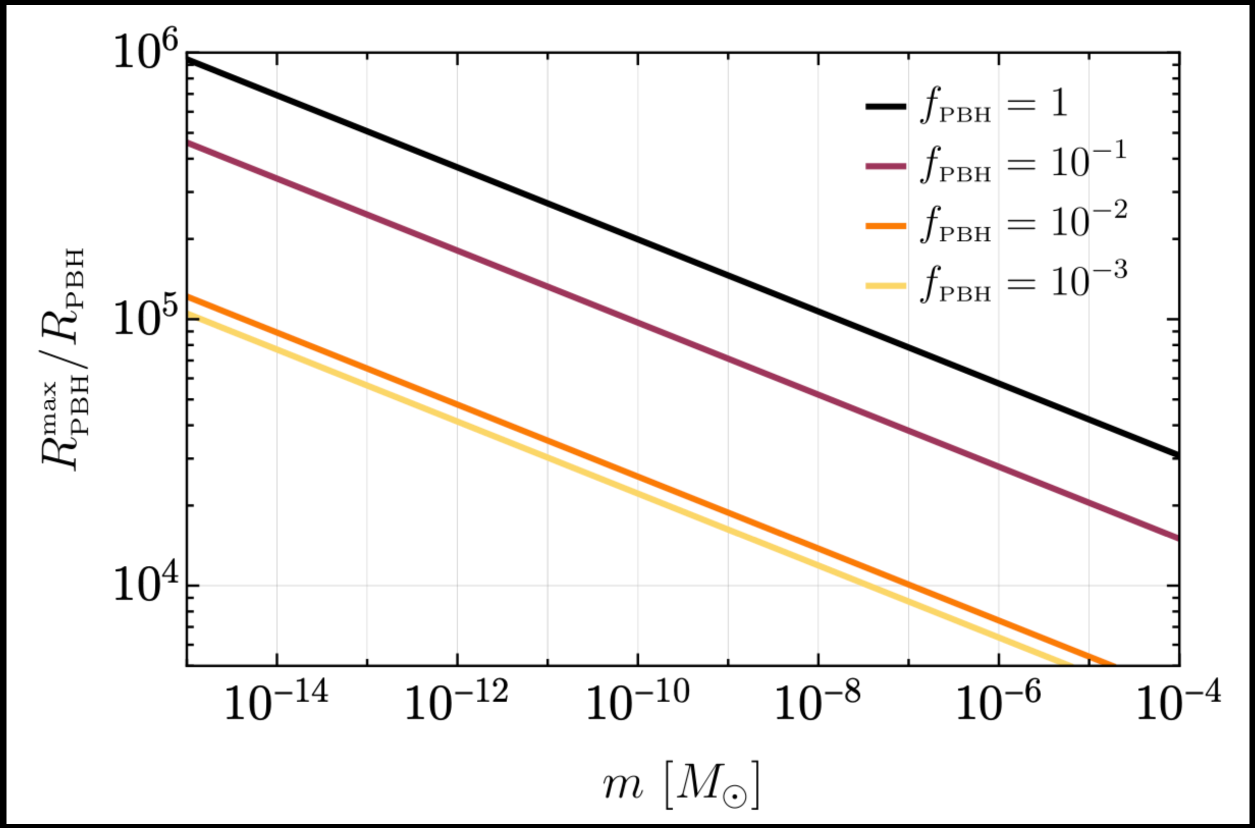

PBH binary formation and evolution

- Late-time dynamical capture: PBH binary formation is induced by GW capture in the present age dense DM environments

  [Bird et al., 2016]
  [Quinlan et al., 1989]

  → subdominant with respect to early universe formation

  → increasingly less relevant for light PBHs

$$\frac{R^{\rm cap}_{\rm PBH}}{R_{\rm PBH}} \sim m_{\rm PBH}^{\frac{265}{777}}$$

- Accretion could affect individual masses, spins and the binary's orbital geometry

  → on light PBH binaries is irrelevant and cannot affect the merger rate

- Clustering at formation due to local non-Gaussianities of primordial perturbations

  [De Luca et al., 2021]

  ↓

  maximum theoretical merger rate

  ↓

  average distance of PBH merger smaller by at most 2 orders of magnitude

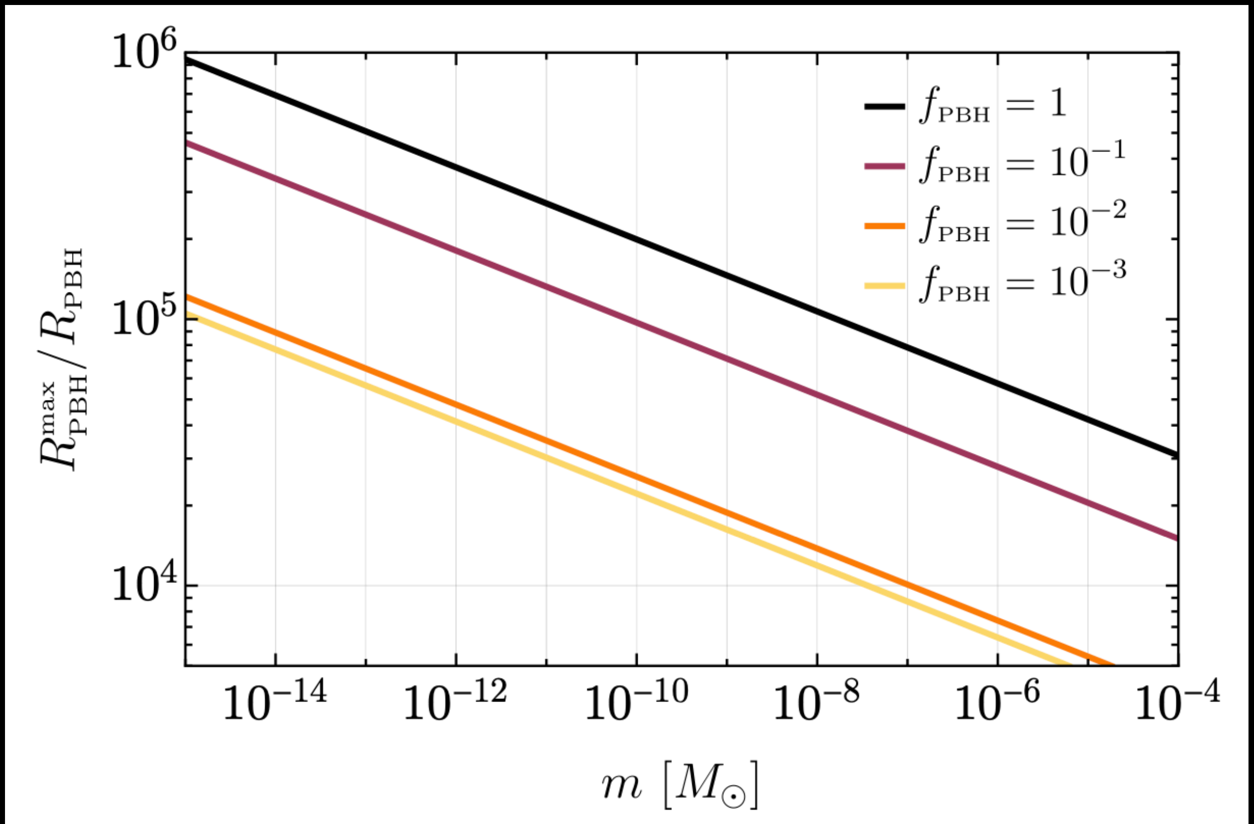

PBH binary formation and evolution

- Local DM enhancement $\longrightarrow$ correction for sources that are closer to the Earth than O(100) kpc

PBH binary formation and evolution

- Local DM enhancement $\longrightarrow$ correction for sources that are closer to the Earth than O(100) kpc

DM density profile:
[Pujolas et al., 2021]

$$\rho(r-\hat{r}) = \begin{cases} \rho_{\rm DM}(r_\odot) & r-\hat{r} < r_\odot \\ \rho_{\rm DM}(r-\hat{r}) & r-\hat{r} > r_\odot \end{cases}$$

$$\rho_{\rm DM}(r) = \frac{\rho_0}{\frac{r}{r_0}\left(1+\frac{r}{r_0}\right)^2}$$

$$\rho_{\rm DM}(r_\odot) = 7.9\times 10^{-3} M_\odot/{\rm pc}^3$$

$$r_0 = 15.6\,{\rm kpc} \qquad r_\odot = 8\,{\rm kpc}$$

PBH binary formation and evolution

- Local DM enhancement ⟶ correction for sources that are closer to the Earth than O(100) kpc

DM density profile: $\rho(r-\hat{r}) = \begin{cases} \rho_{DM}(r_\odot) & r-\hat{r} < r_\odot \\ \rho_{DM}(r-\hat{r}) & r-\hat{r} > r_\odot \end{cases}$

[Pujolas et al., 2021]

$$\rho_{DM}(r) = \frac{\rho_0}{\frac{r}{r_0}\left(1+\frac{r}{r_0}\right)^2}$$

$$\rho_{DM}(r_\odot) = 7.9 \times 10^{-3} M_\odot/\mathrm{pc}^3$$

$$r_0 = 15.6\,\mathrm{kpc} \qquad r_\odot = 8\,\mathrm{kpc}$$

local DM overdensity enhances the merger rate

$$R^{\mathrm{local}}_{\mathrm{PBH}}(r) = \delta(r) R_{\mathrm{PBH}}$$

$$\delta(r) \equiv \frac{\rho_{DM}(r)}{\bar{\rho}_{DM}} \subset (1 \div 2 \times 10^5)$$

PBH binary formation and evolution

- Local DM enhancement ⟶ correction for sources that are closer to the Earth than O(100) kpc

DM density profile: $\rho(r-\hat{r}) = \begin{cases} \rho_{DM}(r_\odot) & r-\hat{r} < r_\odot \\ \rho_{DM}(r-\hat{r}) & r-\hat{r} > r_\odot \end{cases}$

[Pujolas et al., 2021]

$$\rho_{DM}(r) = \frac{\rho_0}{\frac{r}{r_0}\left(1+\frac{r}{r_0}\right)^2}$$

$$\rho_{DM}(r_\odot) = 7.9 \times 10^{-3} M_\odot/\mathrm{pc}^3$$

$$r_0 = 15.6\,\mathrm{kpc} \qquad r_\odot = 8\,\mathrm{kpc}$$

local DM overdensity enhances the merger rate

$$R^{\mathrm{local}}_{\mathrm{PBH}}(r) = \delta(r) R_{\mathrm{PBH}}$$

$$\delta(r) \equiv \frac{\rho_{DM}(r)}{\bar{\rho}_{DM}} \subset (1 \div 2\times 10^5)$$

distance enclosing region with one event per year

$$1 = N_{\mathrm{yr}} = \Delta t \times \int_0^{\mathrm{d_{yr}}} dr\, 4\pi r^2\, R_{\mathrm{PBH}}(r)$$

$$\Delta t = 1\,\mathrm{yr}$$

characteristic size of a region containing at least a merger event per year

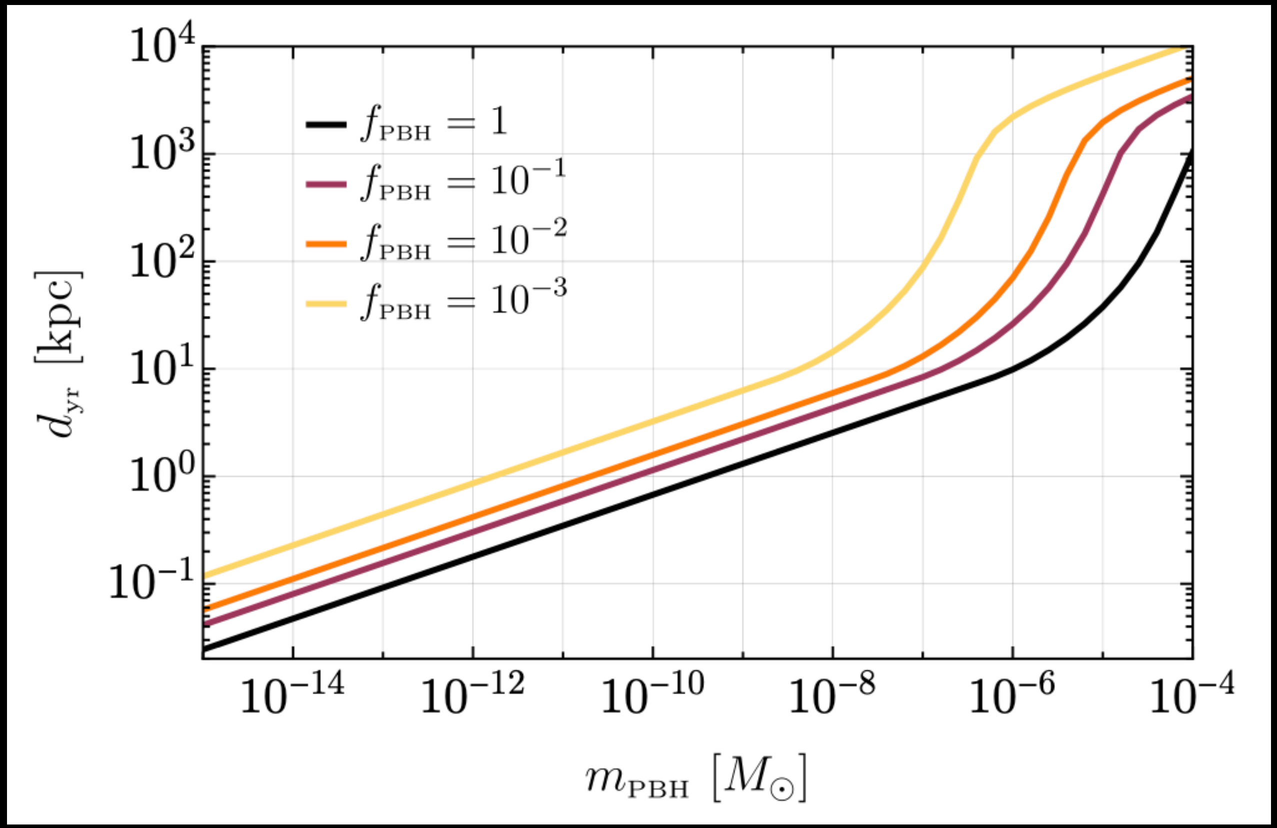

Assumption: narrow PBH mass distribution

PBH inspiral transient signal

- GW signal from a BH inspiral

$$h_i(t) = h_0\, F_i(\theta)\, G_i(t)$$

$$i = +, \times \qquad m_c = \frac{(m_1 m_2)^{3/5}}{(m_1 + m_2)^{1/5}}$$

$$h_0 = \frac{4}{d_L}(G m_c)^{5/3}(\pi f)^{2/3}$$
$$\simeq 9.77 \times 10^{-34} \left(\frac{f}{1\,\mathrm{GHz}}\right)^{2/3} \left(\frac{m_{\mathrm{PBH}}}{10^{-12}\, M_\odot}\right)^{5/3} \left(\frac{d_L}{1\,\mathrm{kpc}}\right)^{-1}$$

- Can the signal be considered approximately monochromatic?

$$N = \frac{f^2}{\dot{f}} \simeq 2.16 \times 10^6 \left(\frac{f}{\mathrm{GHz}}\right)^{-\frac{5}{3}} \left(\frac{m_{\mathrm{PBH}}}{10^{-9}\, M_\odot}\right)^{-\frac{5}{3}} \longrightarrow$$

number of cycles a binary spends at a given frequency

- Time to merger

$$\tau(f) \approx 83\,\mathrm{sec} \left(\frac{m_{\mathrm{PBH}}}{10^{-12}\, M_\odot}\right)^{-5/3} \left(\frac{f}{\mathrm{GHz}}\right)^{-8/3}$$

m_{PBH}	$\tau(1\,\mathrm{GHz})$	$\tau(0.1\,\mathrm{GHz}) - \tau(1\,\mathrm{GHz})$
$10^{-6}\, M_\odot$	9×10^{-9} sec	3.8×10^{-6} sec
$10^{-8}\, M_\odot$	1.8×10^{-5} sec	0.008
$10^{-10}\, M_\odot$	0.038	17.8
$10^{-12}\, M_\odot$	83	38442

PBH inspiral stochastic signal

- Unresolved PBH mergers contribute to a stochastic gravitational wave background

$$h_c \approx \left[\frac{3}{4\pi^2}\left(\frac{H_0}{f}\right)^2 \Omega_{\rm gw}(f)\right]^{1/2} \sim 2\times 10^{-31}\left(\frac{f}{\rm GHz}\right)^{-1}\left(\frac{\Omega_{\rm gw}}{10^{-7}}\right)^{1/2}$$

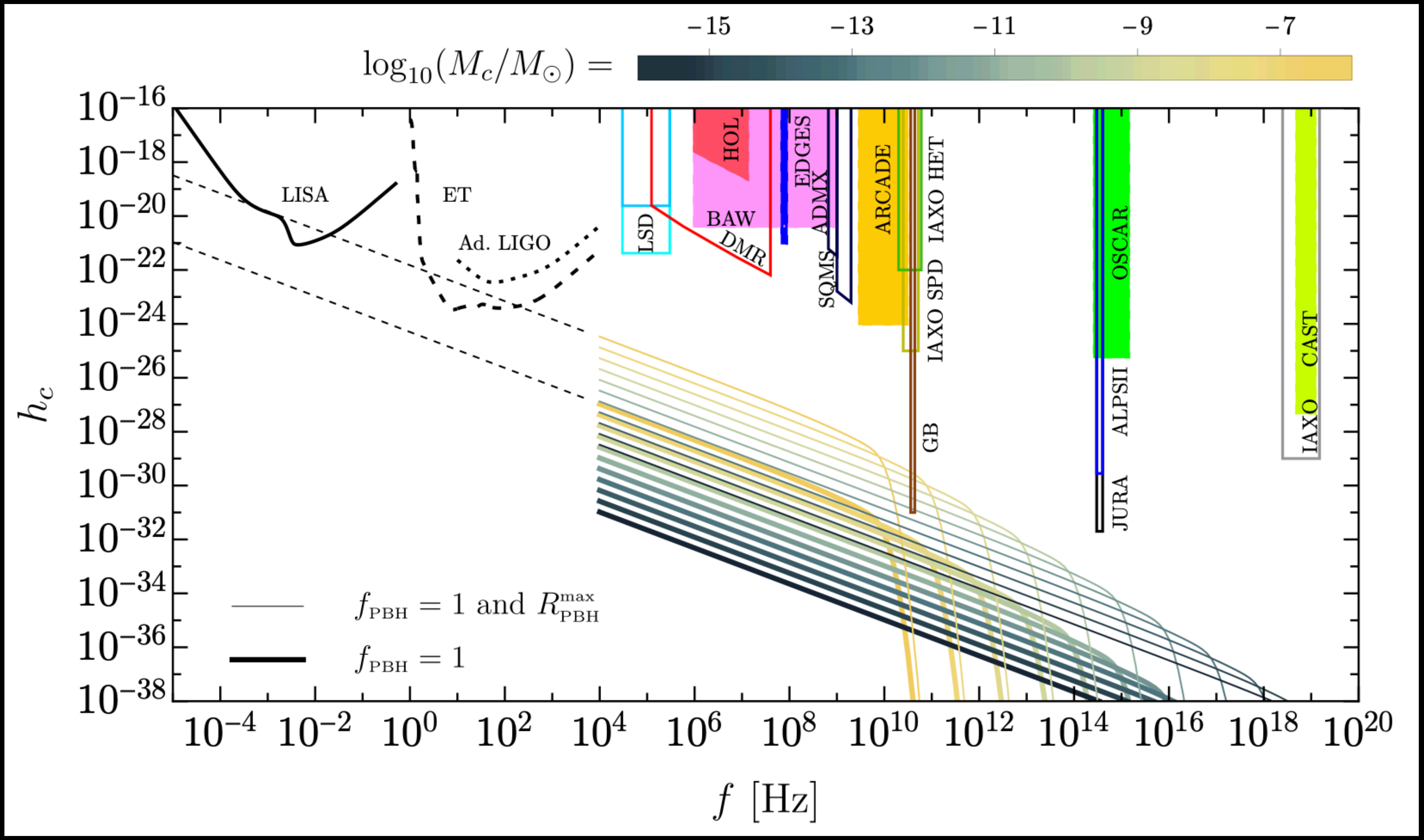

PBH inspiral stochastic signal

- Unresolved PBH mergers contribute to a stochastic gravitational wave background

$$h_c \approx \left[\frac{3}{4\pi^2}\left(\frac{H_0}{f}\right)^2 \Omega_{\rm gw}(f)\right]^{1/2} \sim 2\times 10^{-31}\left(\frac{f}{\rm GHz}\right)^{-1}\left(\frac{\Omega_{\rm gw}}{10^{-7}}\right)^{1/2}$$

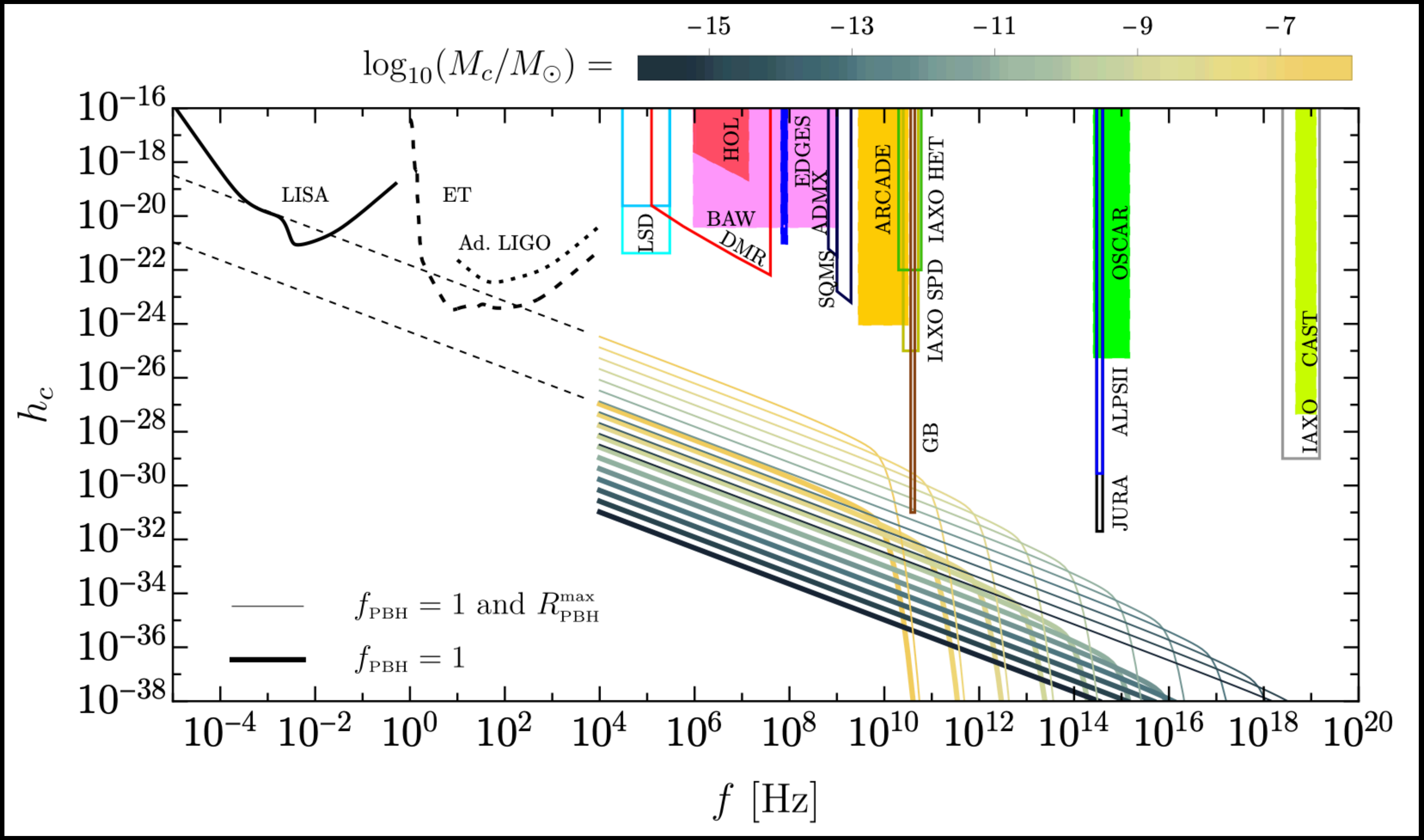

stationary stochastic background ⟶ no issue with time integration

Superradiance

[Arvanitaki et al., 2012]
[Aggarwal et al., 2022]
[Unal, 2023]

- Superradiance requires $1/m_a \sim 2Gm_{\rm PBH}$ axion mass $m_a \simeq \dfrac{M_\odot}{m_{\rm PBH}} 10^{-10}\,{\rm eV}$

Superradiance

[Arvanitaki et al., 2012]
[Aggarwal et al., 2022]
[Unal, 2023]

- Superradiance requires $1/m_a \sim 2Gm_{\rm PBH}$ axion mass $m_a \simeq \frac{M_\odot}{m_{\rm PBH}} 10^{-10}\,{\rm eV}$
- Standard scenario $\longrightarrow$ no spin $\longrightarrow$ no superradiance

Superradiance

[Arvanitaki et al., 2012]
[Aggarwal et al., 2022]
[Unal, 2023]

- Superradiance requires $1/m_a \sim 2Gm_{\rm PBH}$ axion mass $m_a \simeq \frac{M_\odot}{m_{\rm PBH}} 10^{-10}\,{\rm eV}$
- Standard scenario $\longrightarrow$ no spin $\longrightarrow$ no superradiance

$\longrightarrow$ PBH mergers generates a spinning remnant with $\chi \simeq 0.68$ $\longrightarrow$ superradiance

Superradiance

[Arvanitaki et al., 2012]
[Aggarwal et al., 2022]
[Unal, 2023]

- Superradiance requires $1/m_a \sim 2Gm_{\mathrm{PBH}}$ axion mass $m_a \simeq \frac{M_\odot}{m_{\mathrm{PBH}}} 10^{-10}\,\mathrm{eV}$
- Standard scenario $\longrightarrow$ no spin $\longrightarrow$ no superradiance

  $\longrightarrow$ PBH mergers generates a spinning remnant with $\chi \simeq 0.68$ $\longrightarrow$ superradiance
- Axion cloud form around a rotating BH

Superradiance

[Arvanitaki et al., 2012]
[Aggarwal et al., 2022]
[Unal, 2023]

- Superradiance requires $1/m_a \sim 2Gm_{\rm PBH}$ axion mass $m_a \simeq \frac{M_\odot}{m_{\rm PBH}} 10^{-10}\,{\rm eV}$
- Standard scenario $\longrightarrow$ no spin $\longrightarrow$ no superradiance

  $\longrightarrow$ PBH mergers generates a spinning remnant with $\chi \simeq 0.68$ $\longrightarrow$ superradiance

- Axion cloud form around a rotating BH $\longrightarrow$
  - extract rotational energy from BH (superradiance instability)
  - lose energy into GWs

Superradiance

[Arvanitaki et al., 2012]
[Aggarwal et al., 2022]
[Unal, 2023]

- Superradiance requires $1/m_a \sim 2Gm_{\rm PBH}$ axion mass $m_a \simeq \frac{M_\odot}{m_{\rm PBH}} 10^{-10}\,{\rm eV}$
- Standard scenario $\longrightarrow$ no spin $\longrightarrow$ no superradiance

  $\longrightarrow$ PBH mergers generates a spinning remnant with $\chi \simeq 0.68$ $\longrightarrow$ superradiance
- Axion cloud form around a rotating BH $\longrightarrow$
  - extract rotational energy from BH (superradiance instability)
  - lose energy into GWs

  $\downarrow$

  'gravitational atom' with energy levels similar to the hydrogen atom

Superradiance

[Arvanitaki et al., 2012]
[Aggarwal et al., 2022]
[Unal, 2023]

- Superradiance requires $1/m_a \sim 2Gm_{\mathrm{PBH}}$ axion mass $m_a \simeq \dfrac{M_\odot}{m_{\mathrm{PBH}}} 10^{-10}\,\mathrm{eV}$
- Standard scenario ⟶ no spin ⟶ no superradiance

  ⟶ PBH mergers generates a spinning remnant with $\chi \simeq 0.68$ ⟶ superradiance
- Axion cloud form around a rotating BH ⟶
  - extract rotational energy from BH (superradiance instability)
  - lose energy into GWs

  ↓

  'gravitational atom' with energy levels similar to the hydrogen atom
- Axions can transition between levels or annihilate into a graviton

  ↓

  long-lived, monochromatic GW source

Superradiance

[Arvanitaki et al., 2012]
[Aggarwal et al., 2022]
[Unal, 2023]

- Superradiance requires $1/m_a \sim 2Gm_{\rm PBH}$ axion mass $m_a \simeq \dfrac{M_\odot}{m_{\rm PBH}} 10^{-10}\,{\rm eV}$
- Standard scenario $\longrightarrow$ no spin $\longrightarrow$ no superradiance

  $\longrightarrow$ PBH mergers generates a spinning remnant with $\chi \simeq 0.68$ $\longrightarrow$ superradiance

- Axion cloud form around a rotating BH $\longrightarrow$
  - extract rotational energy from BH (superradiance instability)
  - lose energy into GWs

  $\downarrow$

  'gravitational atom' with energy levels similar to the hydrogen atom

- Axions can transition between levels or annihilate into a graviton

  $\downarrow$

  long-lived, monochromatic GW source

$$f \simeq 2\,{\rm MHz}\left(\frac{m_a}{10^{-9}\,{\rm eV}}\right) \sim 2\times10^{2}\,{\rm GHz}\left(\frac{m_{\rm PBH}}{10^{-6}\,M_\odot}\right)^{-1}$$

signal duration $\tau \propto 0.13\,{\rm yr}\left(\dfrac{m_{\rm PBH}}{10^{-6}\,M_\odot}\right)$

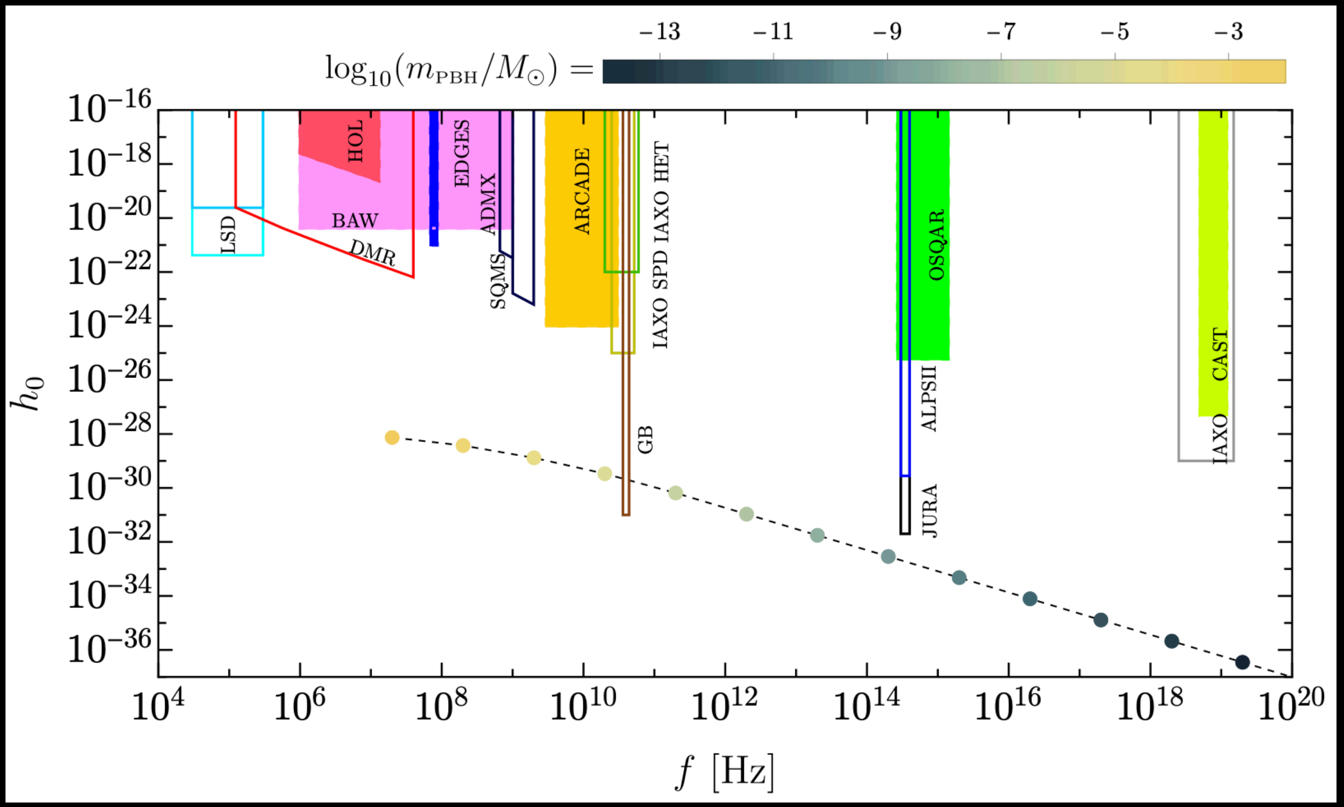

Magnetic conversion

[Ejlli et al., 2014]
[Ringwald et al., 2020]

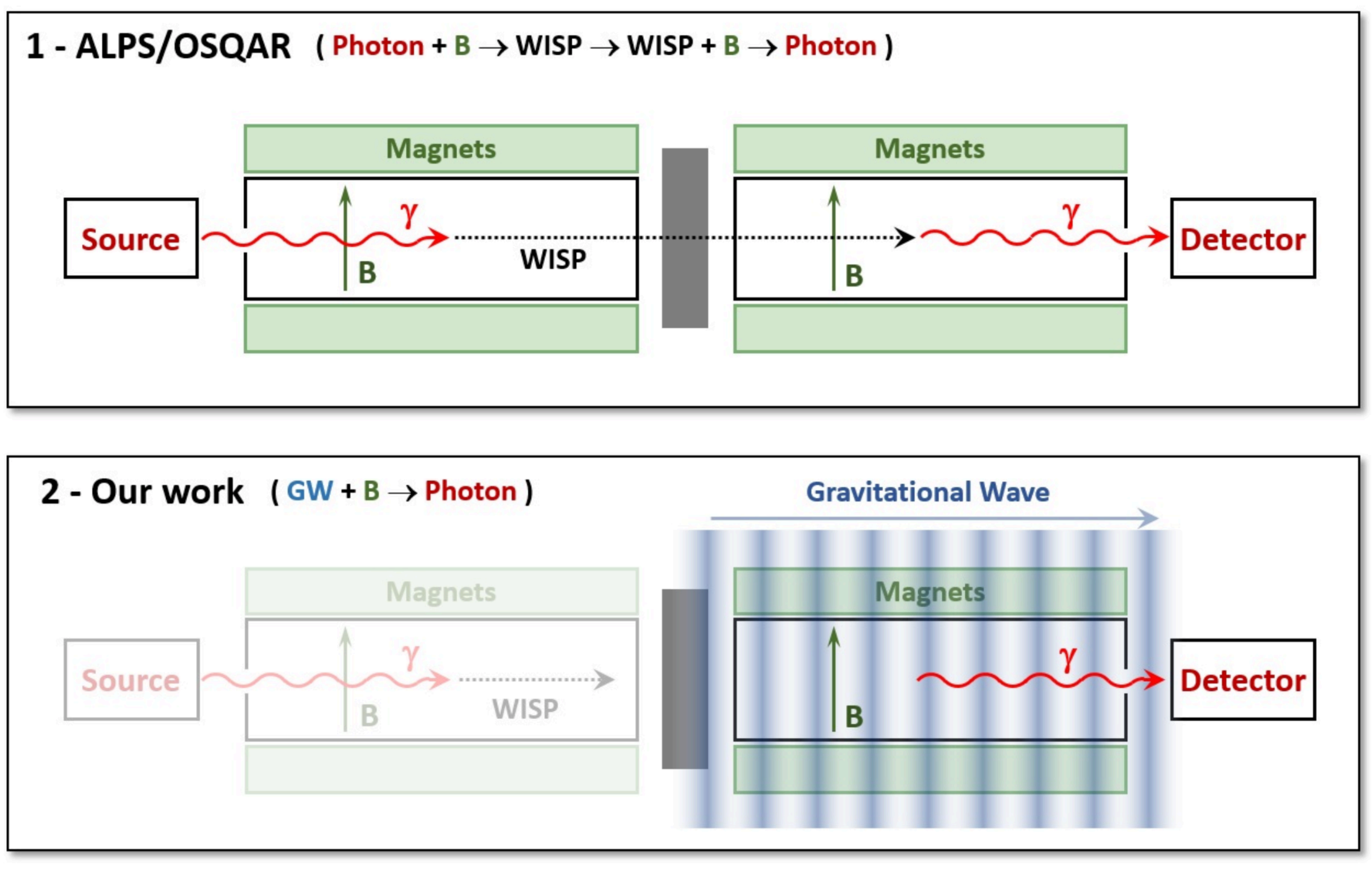

Magnetic conversion

[Boccaletti et al., 1970]
[De Logi et al., 1977]
[Ejlli et al., 2014]
[Ringwald et al., 2020]

- Graviton-photon conversion in a static magnetic field:

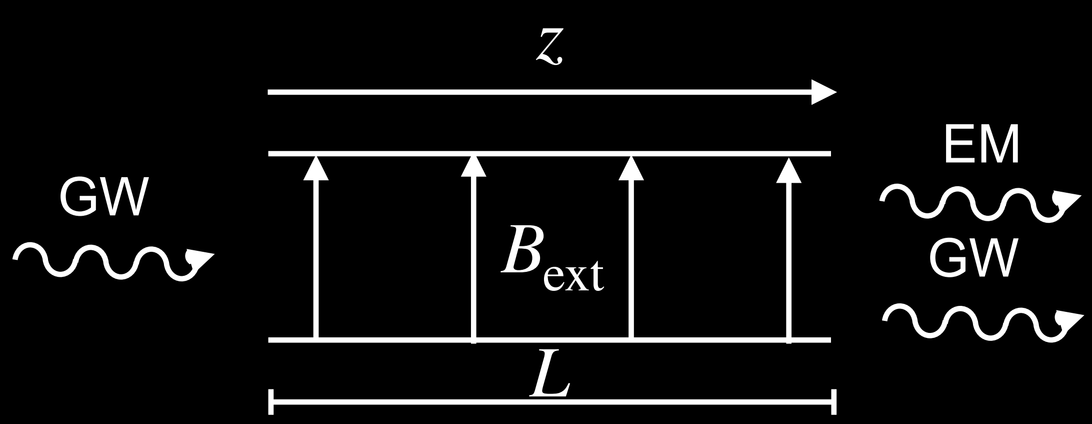

$$\vec{E}^{(1)} \simeq h\vec{B}_{\rm ext}kcz\exp(i(kz-\omega t))$$
$$\vec{B}^{(1)} \simeq h\vec{B}_{\rm ext}kz\exp(i(kz-\omega t))$$

Magnetic conversion

[Boccaletti et al., 1970]
[De Logi et al., 1977]
[Ejlli et al., 2014]
[Ringwald et al., 2020]

- Graviton-photon conversion in a static magnetic field:

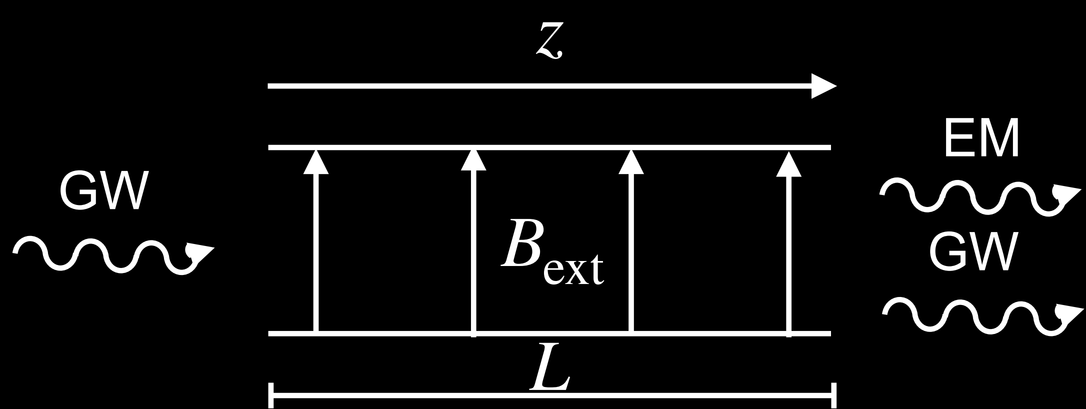

$$\vec{E}^{(1)} \simeq h \vec{B}_{\mathrm{ext}} kcz \exp(i(kz - \omega t))$$
$$\vec{B}^{(1)} \simeq h \vec{B}_{\mathrm{ext}} kz \exp(i(kz - \omega t))$$

quadratic in h

→ power flux density: $u = \dfrac{1}{\mu_0} | \vec{E} \times \vec{B} | \simeq \dfrac{1}{\mu_0}(hB_{\mathrm{ext}}kL)^2 c$

Magnetic conversion

[Boccaletti et al., 1970]
[De Logi et al., 1977]
[Ejlli et al., 2014]
[Ringwald et al., 2020]

- Graviton-photon conversion in a static magnetic field:

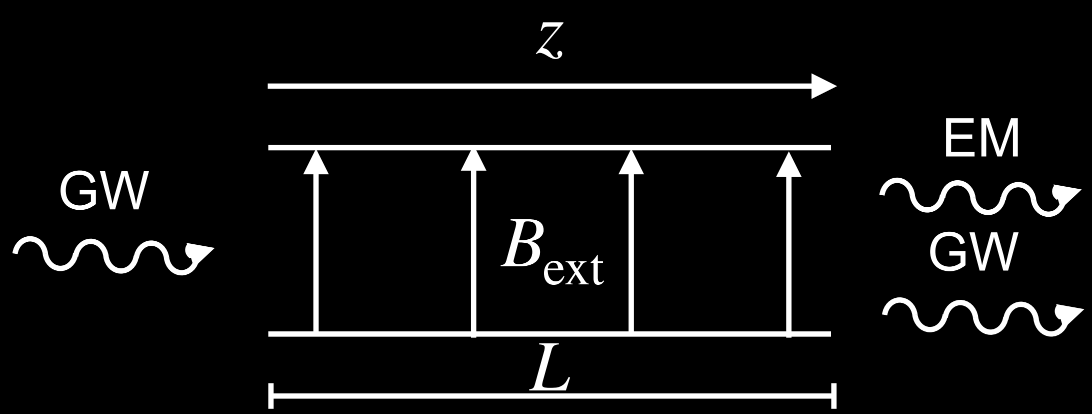

$$\vec{E}^{(1)} \simeq h \vec{B}_{\text{ext}} kcz \exp(i(kz - \omega t))$$

$$\vec{B}^{(1)} \simeq h \vec{B}_{\text{ext}} kz \exp(i(kz - \omega t))$$

quadratic in h

$\longrightarrow$ power flux density: $$u = \frac{1}{\mu_0} |\vec{E} \times \vec{B}| \simeq \frac{1}{\mu_0} (h B_{\text{ext}} k L)^2 c$$

$\longrightarrow$ sensitivity $$h_0 \sim 2.64 \times 10^{-24} \left(\frac{\Delta t}{1\,\text{yr}}\right)^{-\frac{1}{4}} \left(\frac{\Delta f}{10^{11}\,\text{Hz}}\right)^{-\frac{1}{2}} \left(\frac{B}{1\,\text{T}}\right)^{-1} \left(\frac{L}{1\,\text{m}}\right)^{-1} \left(\frac{A}{1\,\text{m}^2}\right)^{-\frac{1}{2}}$$

Magnetic conversion

[Boccaletti et al., 1970]
[De Logi et al., 1977]
[Ejlli et al., 2014]
[Ringwald et al., 2020]

- Graviton-photon conversion in a static magnetic field:

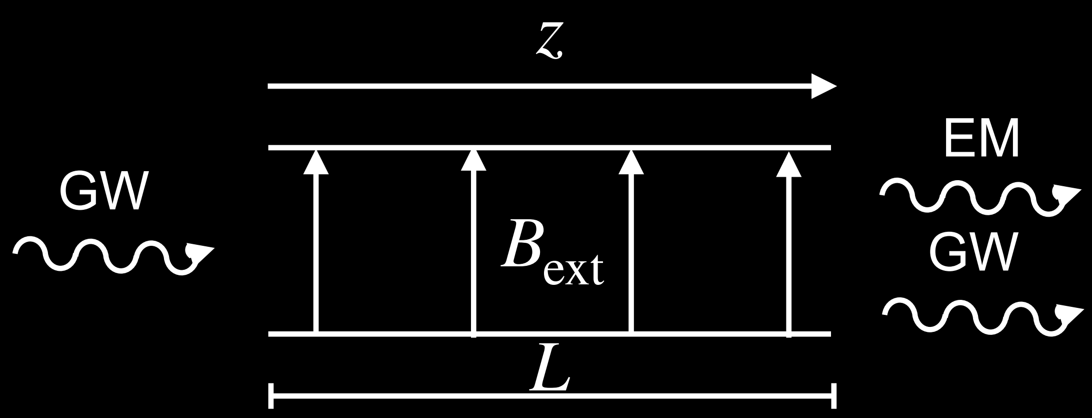

$$\vec{E}^{(1)} \simeq h\vec{B}_{\text{ext}} kcz \exp(i(kz-\omega t))$$
$$\vec{B}^{(1)} \simeq h\vec{B}_{\text{ext}} kz \exp(i(kz-\omega t))$$

quadratic in h

⟶ power flux density: $u = \frac{1}{\mu_0} |\vec{E}\times\vec{B}| \simeq \frac{1}{\mu_0}(hB_{\text{ext}}kL)^2 c$

⟶ sensitivity $h_0 \sim 2.64\times 10^{-24}\left(\frac{\Delta t}{1\,\text{yr}}\right)^{-\frac{1}{4}}\left(\frac{\Delta f}{10^{11}\,\text{Hz}}\right)^{-\frac{1}{2}}\left(\frac{B}{1\,\text{T}}\right)^{-1}\left(\frac{L}{1\,\text{m}}\right)^{-1}\left(\frac{A}{1\,\text{m}^2}\right)^{-\frac{1}{2}}$

- Not possible to detect the chirp phase of light PBHs

$$\Delta t \sim \mathcal{O}(1)\times\frac{1}{f_{\text{ISCO}}} \lesssim 10^{-8}\,\text{sec}$$

Ideal sources:
- superradiance
- early inspiral phase of PBHs
- stochastic backgrounds

- Limitation: coherence between GW and EM requires

$$f \gg \frac{0.45}{\pi}\frac{L}{A} \simeq 4.3\times 10^{7}\,\text{Hz}\left(\frac{L}{1\,\text{m}}\right)\left(\frac{1\,\text{m}}{\sqrt{A}}\right)^2$$

⟶ can only be used at very high frequency

$$f \gg 10^{8}\,\text{Hz}$$

Magnetic conversion

[Barrau et al., 2023]

[Franciolini et al., 2022]

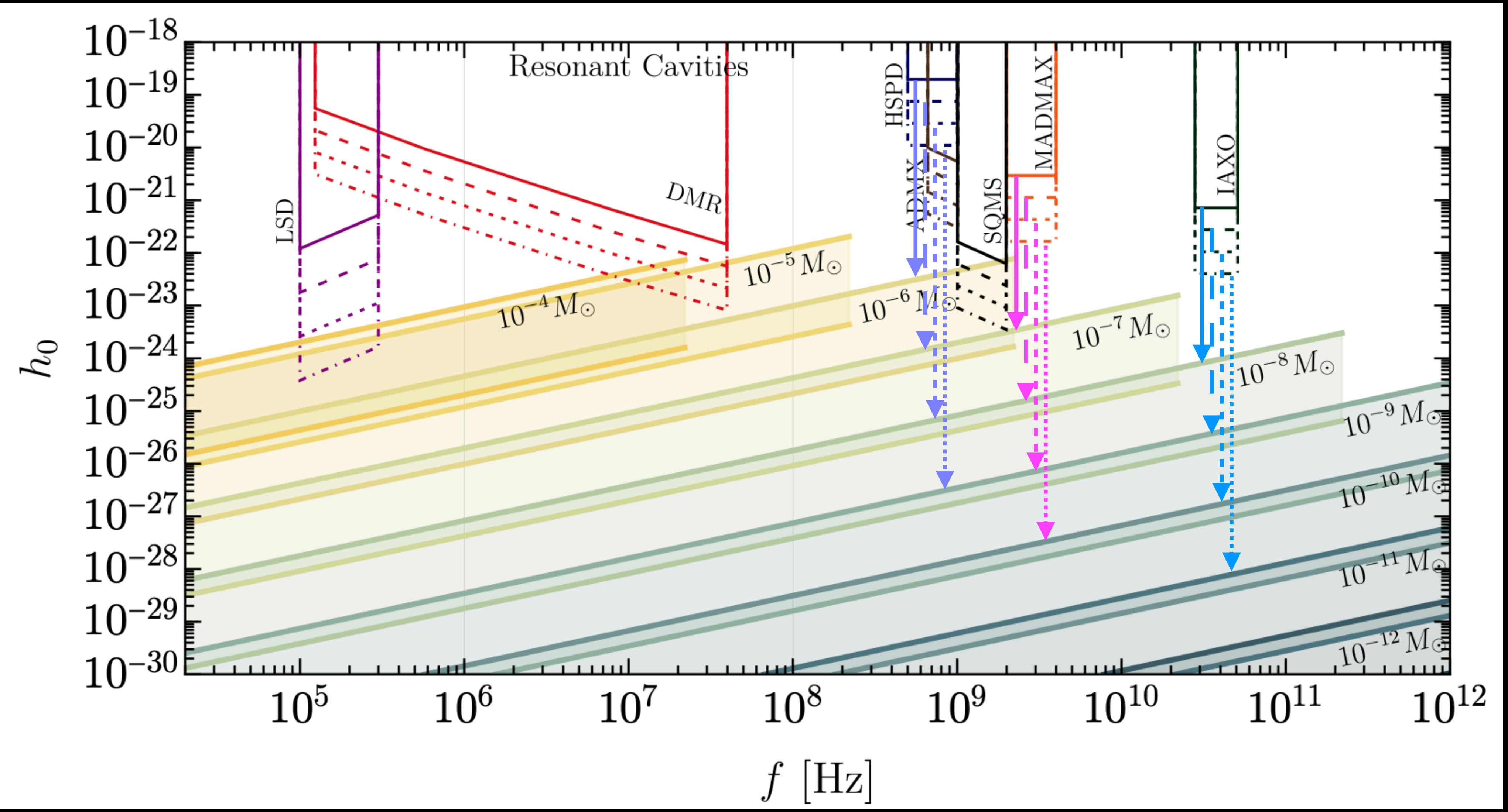

Detector parameters

IAXO	$B = 2.5\,\mathrm{T}$	$L = 20\,\mathrm{m}$	$A = 3.2\,\mathrm{m}^2$	$f \subset (0.5 \div 1) \times 10^9\,\mathrm{Hz}$
MADMAX	$B = 2.5\,\mathrm{T}$	$L = 20\,\mathrm{m}$	$A = 3.2\,\mathrm{m}^2$	$f \subset (2 \div 4) \times 10^9\,\mathrm{Hz}$
HSPD	$B = 1\,\mathrm{T}$	$L = 1\,\mathrm{m}$	$A = 1\,\mathrm{m}^2$	$f \subset (2.8 \div 5.1) \times 10^{10}\,\mathrm{Hz}$

Microwave cavities

[see S. Ellis' talk] [see K. Peter's talk] [Berlin et al., 2022]
[see A. Berlin's talk] [see B. Giaccone's talk] [Berlin et al., 2021]

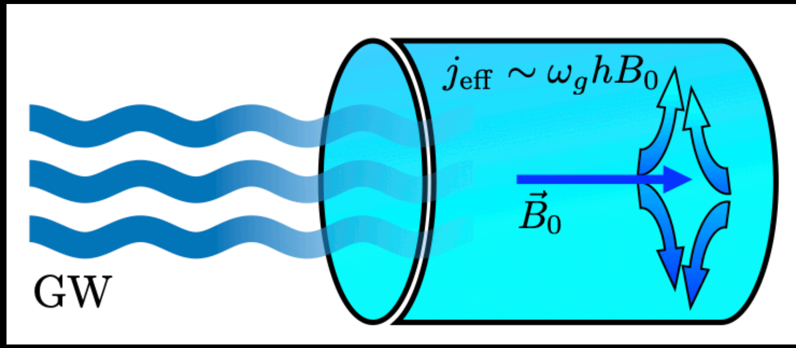

- Sensitivity

$$h_0 = 3\times10^{-22}\left(\frac{0.1}{\eta_n}\right)\left(\frac{8\,\mathrm{T}}{|\mathbf{B}|}\right)\left(\frac{0.1\,\mathrm{m}^3}{\mathrm{Vol}}\right)^{\frac{5}{6}}\left(\frac{10^5}{Q}\right)^{\frac{1}{2}}\times$$
$$\times\left(\frac{\mathrm{T}}{1\,\mathrm{K}}\right)^{\frac{1}{2}}\left(\frac{1\,\mathrm{GHz}}{f}\right)^{\frac{3}{2}}\left(\frac{\Delta f}{10\,\mathrm{kHz}}\right)^{\frac{1}{4}}\left(\frac{1\,\mathrm{min}}{\Delta t}\right)^{\frac{1}{4}}$$

where $\Delta f \simeq f/Q$

- Related experiments: ADMX, HAYSTAC, CAPP, ORGAN, SQMS.

Microwave cavities

[see S. Ellis' talk] [see K. Peter's talk] [Berlin et al., 2022]
[see A. Berlin's talk] [see B. Giaccone's talk] [Berlin et al., 2021]

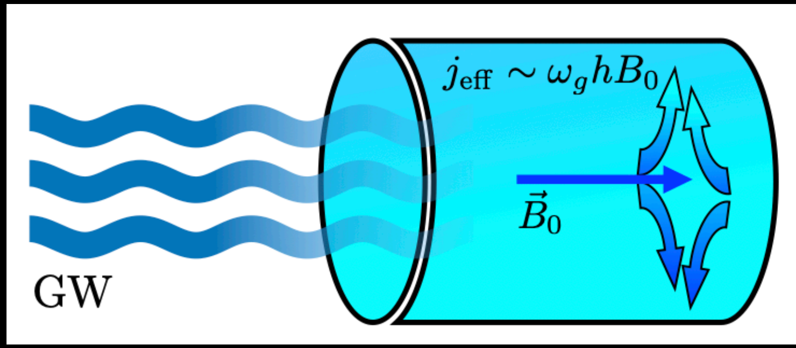

- Sensitivity

$$h_0 = 3\times 10^{-22}\left(\frac{0.1}{\eta_n}\right)\left(\frac{8\,\mathrm{T}}{|\mathbf{B}|}\right)\left(\frac{0.1\,\mathrm{m}^3}{\mathrm{Vol}}\right)^{\frac{5}{6}}\left(\frac{10^5}{Q}\right)^{\frac{1}{2}}\times$$
$$\times\left(\frac{T}{1\,\mathrm{K}}\right)^{\frac{1}{2}}\left(\frac{1\,\mathrm{GHz}}{f}\right)^{\frac{3}{2}}\left(\frac{\Delta f}{10\,\mathrm{kHz}}\right)^{\frac{1}{4}}\left(\frac{1\,\mathrm{min}}{\Delta t}\right)^{\frac{1}{4}}$$

where $\Delta f \simeq f/Q$

- Related experiments: ADMX, HAYSTAC, CAPP, ORGAN, SQMS.
- Signal longer than the ring-up time of the cavity

$m_{\rm PBH} \lesssim 10^{-9}\,M_\odot$ ADMX

$m_{\rm PBH} \lesssim 10^{-10}\,M_\odot$ SQMS

Microwave cavities

[see S. Ellis' talk] [see K. Peter's talk] [Berlin et al., 2022]
[see A. Berlin's talk] [see B. Giaccone's talk] [Berlin et al., 2021]

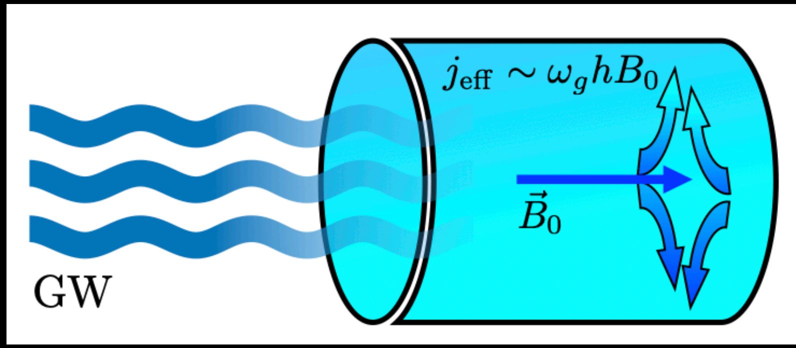

- Sensitivity

$$h_0 = 3\times 10^{-22}\left(\frac{0.1}{\eta_n}\right)\left(\frac{8\,\mathrm{T}}{|\mathbf{B}|}\right)\left(\frac{0.1\,\mathrm{m}^3}{\mathrm{Vol}}\right)^{\frac{5}{6}}\left(\frac{10^5}{Q}\right)^{\frac{1}{2}}\times$$
$$\times\left(\frac{\mathrm{T}}{1\,\mathrm{K}}\right)^{\frac{1}{2}}\left(\frac{1\,\mathrm{GHz}}{f}\right)^{\frac{3}{2}}\left(\frac{\Delta f}{10\,\mathrm{kHz}}\right)^{\frac{1}{4}}\left(\frac{1\,\mathrm{min}}{\Delta t}\right)^{\frac{1}{4}}$$

where $\Delta f \simeq f/Q$

- Related experiments: ADMX, HAYSTAC, CAPP, ORGAN, SQMS.
- Signal longer than the ring-up time of the cavity

$m_{\rm PBH} \lesssim 10^{-9}\,M_\odot$ ADMX

$m_{\rm PBH} \lesssim 10^{-10}\,M_\odot$ SQMS

Resonant LC circuits

[Domcke et al., 2022]

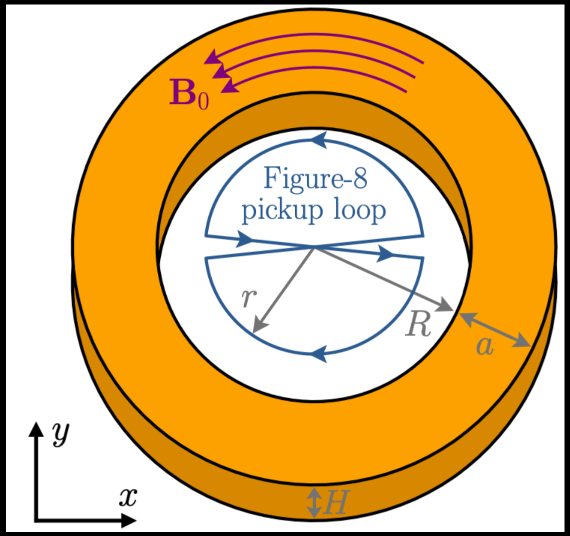

- Suitable to probe the chirp phase at $f \sim 1\,\mathrm{MHz}$ for $m_{\rm PBH} \simeq 10^{-5}\,M_\odot$.

Microwave cavities

[see S. Ellis' talk] [see K. Peter's talk] [Berlin et al., 2022]
[see A. Berlin's talk] [see B. Giaccone's talk] [Berlin et al., 2021]

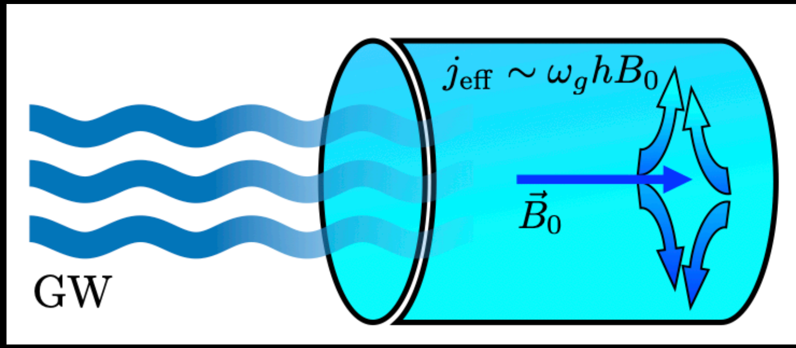

- Sensitivity

$$h_0 = 3\times 10^{-22}\left(\frac{0.1}{\eta_n}\right)\left(\frac{8\,\mathrm{T}}{|\mathbf{B}|}\right)\left(\frac{0.1\,\mathrm{m}^3}{\mathrm{Vol}}\right)^{\frac{5}{6}}\left(\frac{10^5}{Q}\right)^{\frac{1}{2}}\times$$
$$\times\left(\frac{\mathrm{T}}{1\,\mathrm{K}}\right)^{\frac{1}{2}}\left(\frac{1\,\mathrm{GHz}}{f}\right)^{\frac{3}{2}}\left(\frac{\Delta f}{10\,\mathrm{kHz}}\right)^{\frac{1}{4}}\left(\frac{1\,\mathrm{min}}{\Delta t}\right)^{\frac{1}{4}}$$

where $\Delta f \simeq f/Q$

- Related experiments: ADMX, HAYSTAC, CAPP, ORGAN, SQMS.
- Signal longer than the ring-up time of the cavity

$m_{\rm PBH} \lesssim 10^{-9}\, M_\odot$ ADMX

$m_{\rm PBH} \lesssim 10^{-10}\, M_\odot$ SQMS

Resonant LC circuits

[Domcke et al., 2022]

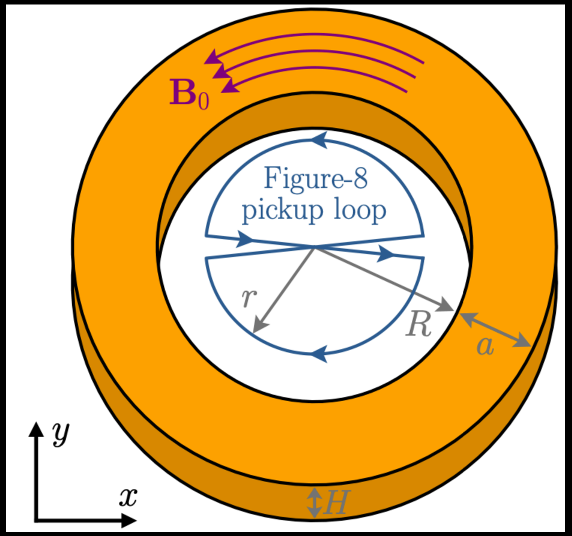

- Suitable to probe the chirp phase at $f \sim 1\,\mathrm{MHz}$ for $m_{\rm PBH} \simeq 10^{-5}\, M_\odot$.
- Related experiments are ADMX SLIC, ABRACADABRA, BASE, SHAFT, WISPLC.
- Sensitivity scales as $\mathrm{Vol}^{7/6}$

$\longrightarrow$ interesting prospects with DMRadio

Microwave cavities & Resonant LC circuits

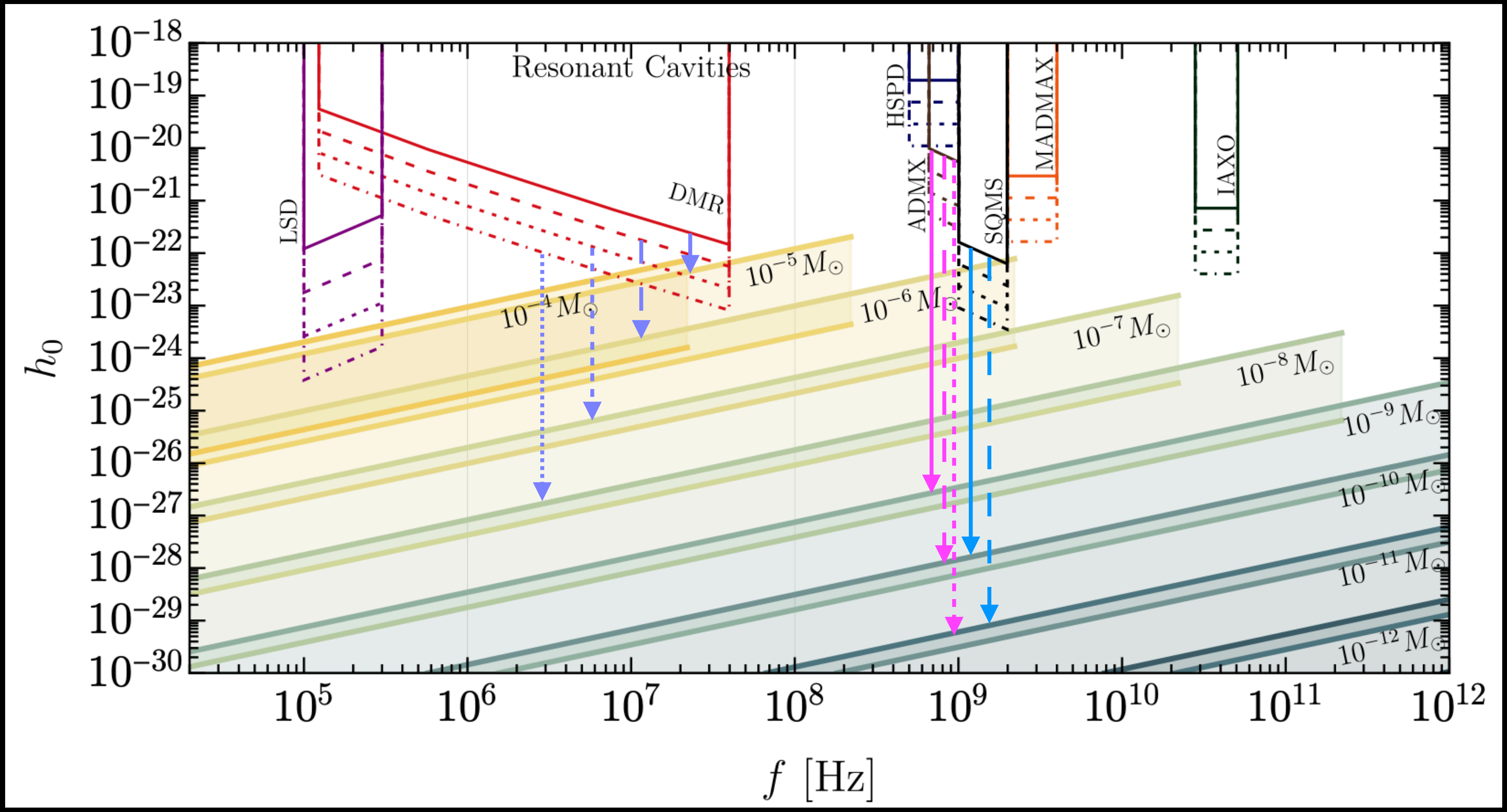

Detector parameters

DMR	$B = 4\,\mathrm{T}$	$\mathrm{Vol} = 100\,\mathrm{m}^3$			$f \subset (0.1 \div 30)\,\mathrm{MHz}$
ADMX	$B = 7.5\,\mathrm{T}$	$\mathrm{Vol} = 136\,\mathrm{L}$	$\mathrm{T} = 0.6\,\mathrm{K}$	$\mathrm{Q} = 8 \times 10^4$	$f \subset (0.65 \div 1.02)\,\mathrm{GHz}$
SQMS	$B = 5\,\mathrm{T}$	$\mathrm{Vol} = 100\,\mathrm{L}$	$\mathrm{T} = 1\,\mathrm{K}$	$\mathrm{Q} = 10^6$	$f \subset (1 \div 2)\,\mathrm{GHz}$

Conclusions

- The Ultra-High-Frequency band is very well motivated from the theoretical point of view and worth studying.
- Technological progress is still necessary in order to make a first GW detection.
- A few detector proposals appeared after we published our paper.

Conclusions

- The Ultra-High-Frequency band is very well motivated from the theoretical point of view and worth studying.
- Technological progress is still necessary in order to make a first GW detection.
- A few detector proposals appeared after we published our paper.

https://indico.cern.ch/event/1257532/

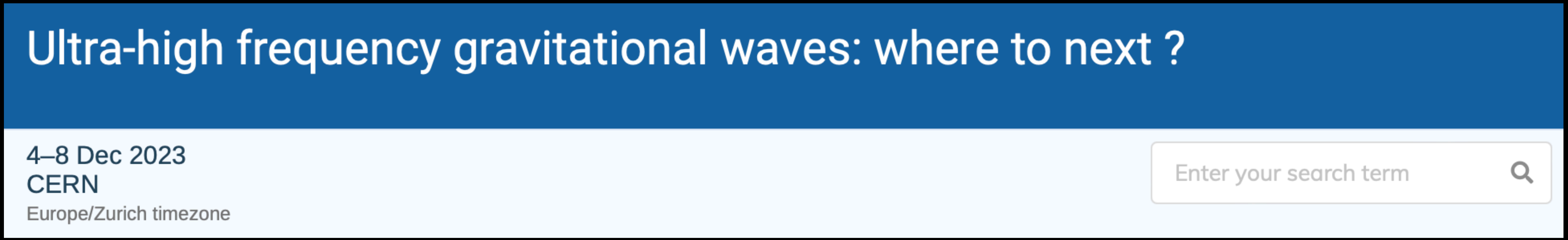

Thank you!